Chapter 1

Introduction

General Relativity (GR) is founded on the revolutionary idea that space and time are merely parts of a greater, unified whole: spacetime. Furthermore, the force we know as gravity results from the bending and stretching of the geometry of spacetime by its energetic contents. GR is notorious for its mathematical complexity and subtlety, meaning that an intuitive understanding of a spacetime is difficult. One of the best approaches to studying the properties of a given spacetime is to consider its geodesic structure—that is, to consider the motion of unaccelerated, "free-falling" particles. This report presents the results of such a study into two important spacetimes—the Kerr solution for a rotating black hole, and the Robertson-Walker solution for a homogeneous universe.

1.1 Geodesics in General Relativity

We begin with a general intoduction to GR and geodesics[1]. Note that throughout this report, the speed of light c has been set to unity unless explicitly reintroduced. Carroll (2004) reduces GR to the following two statements:

1. Spacetime is a curved pseudo-Riemannian manifold with a metric of signature[2] $(-+++)$.
2. The relationship between matter and the curvature of spacetime is contained in the equation:

$$R_{ab} - \frac{1}{2}Rg_{ab} = 8\pi G T_{ab} \tag{1.1}$$

   where G is Newton's gravitational constant, which we now set to unity unless explicitly reintroduced.

The first statement says that gravity does not move objects via a Newtonian force that causes them to deviate from straight line motion. Instead, gravity makes straight lines curve! The second statement says that the geometry of spacetime (encapsulated by the Ricci tensor R_{ab}, Ricci scalar R and metric tensor g_{ab}) is curved by the presence of energy, represented by the stress-energy tensor T_{ab}. Conceptually, Equation (1.1) states that:

$$\textbf{Geometry = Energy} \tag{1.2}$$

The full details of pseudo-Riemannian geometry are not needed here, so we will not elaborate on the terms in Equation (1.1). However, it will be useful to gain an intuitive understanding of the metric tensor g_{ab}. In a given coordinate system $x^a = (x^0, x^1, x^2, x^3)$ the invariant spacetime interval between two nearby events is:

$$\mathrm{d}s^2 = g_{ab}\mathrm{d}x^a\mathrm{d}x^b \tag{1.3}$$

using the Einstein summation convention[3]. We can begin to understand this quantity by considering special cases:

[1] There are a great many introductions to GR available, including D'Inverno (1992), Carroll (2004) and Hobson et al. (2005).

[2] This work will use the $(-+++)$ signature, Latin letters for spacetime indices $(a, b, \ldots = 0, 1, 2, 3)$ and Greek letters $(\alpha, \beta \ldots = 1, 2, 3)$ for spatial indices.

[3] Repeated indices are automatically summed over.

- If $\mathrm{d}s^2 > 0$, then the interval is **spacelike**. This means that it is possible for an observer (moving with the correct velocity) to observe that the two events occur at the same time. In this case, $\sqrt{\mathrm{d}s^2}$ is the **proper distance** between the two events, and (1.3) is simply a generalisation of pythagorus theorem.
- If $\mathrm{d}s^2 < 0$, then the interval is **timelike**. This means that it is possible for an observer (moving with the correct velocity) to observe that the two events occur at the same spatial location. In this case, $\sqrt{-\mathrm{d}s^2}$ is the **proper time** between the two events.
- If $\mathrm{d}s^2 = 0$, then the interval is **null**. This means that light emitted at the first event will be observed at the second event. Null intervals define the **light cone** of an event.

A physical observer can only experience two events that are timelike separated. The trajectory of an observer through spacetime is called its **worldline** and consists of a one-parameter set of all the events that the observer experiences: $x^a = x^a(\lambda)$. The parameter λ is known as the affine parameter. In the case of null geodesics (i.e. trajectories comprising entirely of null intervals, which light would follow), λ has no physical interpretation, while in the case of timelike and spacelike geodesics, it is chosen to be the spacelike interval s. This means that timelike geodesics are parameterised by the proper time (τ) shown on a clock following the given trajectory.

The metric tensor determines the geometry of spacetime, and since the trajectories of free-falling particles are determined by the geometry of spacetime, we expect to find a mathematical relationship between the metric tensor and the trajectory of an unaccelerated particles. Since unaccelerated particles follow the geodesics of spacetime, this relationship can be found by extremising the spacetime interval between two events i.e.

$$\int \mathrm{d}s = \int \sqrt{g_{ab}\frac{\mathrm{d}x^a}{\mathrm{d}\lambda}\frac{\mathrm{d}x^b}{\mathrm{d}\lambda}}\mathrm{d}\lambda \tag{1.4}$$

$$= \int \sqrt{g_{ab}x'^a x'^b}\mathrm{d}\lambda \tag{1.5}$$

where $x'^a = \frac{\mathrm{d}x^a}{\mathrm{d}\lambda}$ is the 4-velocity. We now have a problem that can be easily handled by the Euler-Lagrange equation (see, among others, D'Inverno, 1992, pg. 82). The result is a set of four, second-order equations for $x^a = x^a(\lambda)$, known collectively as the **geodesic equation**:

$$\frac{\mathrm{d}^2x^a}{\mathrm{d}\lambda^2} + \Gamma^c_{\ ba}\frac{\mathrm{d}x^a}{\mathrm{d}\lambda}\frac{\mathrm{d}x^b}{\mathrm{d}\lambda} = 0 \tag{1.6}$$

where $\Gamma^c_{\ ba}$ is the Christoffel symbol, which is calculated from the derivatives of the metric tensor:

$$\Gamma^c_{\ ba} = \frac{1}{2}g^{ad}\left(\partial_b g_{dc} + \partial_c g_{db} - \partial_d g_{bc}\right) \tag{1.7}$$

where

$$\partial_a = \frac{\partial}{\partial x^a} \tag{1.8}$$

One more equation is needed, which follows from Equation (1.3). If we divide this equation by $\mathrm{d}\lambda$, we find that:

$$g_{ab}x'^a x'^b = q = \begin{cases} -1 & \text{for timelike geodesics} \\ 0 & \text{for null geodesics} \\ +1 & \text{for spacelike geodesics} \end{cases} \tag{1.9}$$

We will be seeking and interpreting solutions to Equation (1.6) subject to the contraint Equation (1.9).

1.2 The Kerr Metric

1.2.1 Properties of the Kerr Metric

This section follows the discussion and notation of O'Neill (1995). We start with the Schwarzschild metric. In 1916, Schwarzschild discovered the solution to Einstein's equations in the case of a spacetime that is:

- Empty (i.e. a vacuum solution: $T_{ab} = 0$)
- Spherically-symmetric
- Stationary (i.e. no explicit time dependence $\partial_0 g_{ab} = \partial_t g_{ab} = 0$)
- Static (i.e. time symmetric $g_{0\alpha} = 0$).

The Schwarzschild metric descibes the spacetime surrounding a spherical, non-rotating mass. It was the first exact solution of Einstein's equations. In spherical polar coordinates $[(x^0, x^1, x^2, x^3) = (t, r, \theta, \phi)]$, its metric tensor is given in matrix form by:

$$g_{ab} = \begin{pmatrix} -1 + \frac{2M}{r} & 0 & 0 & 0 \\ 0 & \left(1 - \frac{2M}{r}\right)^{-1} & 0 & 0 \\ 0 & 0 & r^2 & 0 \\ 0 & 0 & 0 & r^2 \sin^2\theta \end{pmatrix} \tag{1.10}$$

where M is the mass of the object. Equivalently, we can specify the line element using Equation (1.3):

$$\mathrm{d}s^2 = -\left(1 - \frac{2M}{r}\right)\mathrm{d}t^2 + \left(1 - \frac{2M}{r}\right)^{-1}\mathrm{d}r^2 + r^2(\mathrm{d}\theta^2 + \sin^2\theta\,\mathrm{d}\phi^2) \tag{1.11}$$

Note that by setting the mass equal to zero we return to the flat Minkowskian spacetime of Special Relativity.

Large astronomical bodies are likely to be rotating, so a more general solution is needed. To find it, we need to weaken some of our assumptions: spherical symmetry will be weakened to axisymmetry, since the object will have a preferred axis of rotation; and the solution will not be static, as reversing the direction of time will reverse the direction of rotation. The solution conforming to these assumptions was first discovered by Kerr in 1963, and is appropriately named the Kerr metric:

$$g_{ab} = \begin{pmatrix} -1 + \frac{2Mr}{\rho^2} & 0 & 0 & \frac{-2Mra\sin^2\theta}{\rho^2} \\ 0 & \frac{\rho^2}{\Delta} & 0 & 0 \\ 0 & 0 & \rho^2 & 0 \\ \frac{-2Mra\sin^2\theta}{\rho^2} & 0 & 0 & \left(r^2 + a^2 + \frac{2Mra^2\sin^2\theta}{\rho^2}\right)\sin^2\theta \end{pmatrix} \tag{1.12}$$

where M is the mass of the rotating object, a is the angular momentum per unit mass, which can be taken to be positive, and

$$\rho^2 = r^2 + a^2\cos^2\theta \tag{1.13}$$

$$\Delta = r^2 - 2Mr + a^2 \tag{1.14}$$

The metric is written in Boyer-Lindquist coordinates. Again we can consider the line element corresponding to this metric:

$$\mathrm{d}s^2 = -\left(1 - \frac{2Mr}{\rho^2}\right)\mathrm{d}t^2 + \frac{\rho^2}{\Delta}\mathrm{d}r^2 + \rho^2\mathrm{d}\theta^2 + \left(r^2 + a^2 + \frac{2Mra^2\sin^2\theta}{\rho^2}\right)\sin^2\theta\,\mathrm{d}\phi^2 - \frac{4Mra\sin^2\theta}{\rho^2}\,\mathrm{d}t\,\mathrm{d}\phi \tag{1.15}$$

The following properties of Kerr spacetime will be useful in what follows (see D'Inverno (1992), O'Neill (1995) and Hobson et al. (2005) for a more detailed and rigorous discussion.)

Slow and Fast Kerr: As we vary the parameter a, a profound change occurs at the extreme value $a^2 = M^2$. Following O'Neill (1995), we can fix the following terminology:

- $a^2 = 0$ gives Schwarzschild spacetime, as expected.
- $0 < a^2 < M^2$ gives slowly rotating Kerr spacetime, known in short as *slow Kerr*.
- $a^2 = M^2$ gives *extreme Kerr spacetime*.
- $a^2 > M^2$ gives rapidly rotating Kerr spacetime, or *fast Kerr*. As discussed in D'Inverno (1992), the spacetime singularity in fast Kerr spacetime is naked—that is, it is not hidden from the outside universe by an event horizon. The consequences of such a scenario are so bizarre that Penrose has proposed the cosmic censorship hypothesis, which would forbid the existence of naked singularities.

Fast Kerr spacetimes are unlikely to be relevent in astrophysical contexts, so we will not examine them in this report. When we speak of Kerr spacetime, we mean slow and extreme Kerr spacetime ($0 < a^2 \leq M^2$). To avoid countless exceptions, we will not consider Schwarzschild spacetime to be in the Kerr family.

Singularities and Horizons: Kerr spacetime contains an intrinsic singularity when $\rho = 0$. It follows from Equation (1.13) that $r = \cos\theta = 0$. However, unlike Schwarzschild spacetime, the Kerr metric does not fail at $r = 0$ and the singularity is not a single point. Instead, the singularity is a ring in the equatorial plane.

Kerr spacetime also contains a number of coordinate singularities and peculiarities. The most tame of these is the failure of spherical coordinates on the axis of rotation when $\sin\theta = 0$. While the absence of spherical symmetry means that the axis is physically and geometrically unique, we can extend the Kerr metric to account for these coordinate problems (see O'Neill, 1995, pg. 64).

Of more interest physically are the stationary limit surfaces and the event horizons of the Kerr metric. The **stationary limit surfaces** are defined by:

$$g_{tt} = 0 \qquad \Rightarrow \qquad r_{S_\pm} = M \pm \sqrt{M^2 - a^2\cos^2\theta} \tag{1.16}$$

Since we have confined our attention to $0 < a^2 \leq M^2$, we have two stationary limit surfaces surrounding the central singularity, the inner surface (S_-) being completely contained inside the outer surface (S_+). We will not be concerned with the inner structure of the Kerr black hole, so we only need to note that inside S_+ no particle can remain at fixed (r, θ, ϕ). They must rotate around the black hole.

The Kerr spacetimes we will consider also contain **event horizons** that mark the "point of no return". There are two event horizons (at $r = r_\pm$) defined by:

$$g_{rr} \to \infty \qquad \Rightarrow \qquad \Delta \to 0 \qquad \Rightarrow \qquad r_\pm = M \pm \sqrt{M^2 - a^2} \tag{1.17}$$

Once again, only the outer horizon will interest us here. It lies inside the outer stationary limit surface, with the two touching at the poles ($\theta = 0, \pi$). Boyer-Lindquist coordinates fail at the event horizons, meaning that they are "bad coordinates" for following the trajectories of particles into the black hole. The Kerr event horizon works in the same way as a Schwarzschild event horizon—it can only be crossed in one direction, so that the future light cone lies entirely on the inside of the surface. Particles must continue falling toward the centre. Note that for an extreme kerr black hole, the two event horizons coincide at $r = M$.

The region between S_+ and r_+ is known as the **ergosphere**. Within the ergosphere, particles must rotate with the black hole but need not fall through the event horizon. In other words, the particle can escape the gravitational effects of the black hole but not its rotational effects.

We can also define the **innermost stable circular orbit** (also known as the minimal stable orbit r_{ms})—the innermost radius at which a massive particle can maintain a stable orbit around the black hole in the equatorial plane. It is given by the solution to the following equation (Hobson et al., 2005):

$$r_{ms}^2 - 6Mr_{ms} - 3a^2 \mp 8a\sqrt{Mr_{ms}} = 0 \tag{1.18}$$

where the upper sign corresponds to a counter-rotating orbit and the lower sign to a co-rotating orbit. The above equation can be turned into a quartic polynomial and solved by standard methods, but the results are messy. The results of solving this equation numerically can be found in (Hobson et al., 2005). The results can be summarised as follows: for $a = 0$, we have the Schwarzschild result that $r_{ms} = 6M$. In the counter-rotating case, r_{ms} increases approximately linearly with a up to $r_{ms} = 9M$ in the case of an extreme Kerr black hole ($a = M$). In the co-rotating case, r_{ms} decreases with a down to $r_{ms} = M$ in the case of an extreme Kerr black hole. Thus, for an extreme Kerr black hole, the innermost stable circular orbit and the outer event horizon coincide.

The **photon sphere** is defined analogously to Schwarzschild spacetime (although in Kerr spacetime it isn't a perfect sphere). Photons in the equatorial plane can orbit the black hole at a radius of (Hobson et al., 2005):

$$r_c = 2M\left(1 + \cos\left[\frac{2}{3}\cos^{-1}\left(\pm\frac{a}{M}\right)\right]\right) \tag{1.19}$$

where again the upper sign corresponds to a counter-rotating orbit and the lower sign to a co-rotating orbit. In short, for $a = 0$, we have the Schwarzschild result that $r_c = 3M$. In the counter-rotating case, r_c increases approximately linearly with a up to $r_c = 4M$ in the case of an extreme Kerr black hole ($a = M$). In the co-rotating case, r_{ms} decreases with a down to $r_c = M$ in the case of an extreme Kerr black hole. Thus, for an extreme Kerr black hole, the photon sphere, the innermost stable circular orbit and the outer event horizon coincide.

1.2.2 Geodesics in Kerr Spacetime

For the Kerr metric, we solve the second-order system of equations (1.6) for four functions of the affine parameter. There are 3 obvious constants of the motion - the constraint equation (1.9) defines the constant q, and the other two come from the fact that time t and azimuthal angle ϕ are absent from the Lagrangian, meaning that their conjugate momenta (energy E and the component of the angular momentum along the rotation axis L respectively) are conserved. Ordinarily, three constants of the motion is not enough to reduce this second-order system for four functions down to a first order system. However, Carter (1968) showed that the Hamilton-Jacobi equation of motion is separable, which generates the fourth constant of the motion (known as Carter's constant K). Thus, the equations of motion for geodesics in Kerr spacetime reduce to the following first-order system of equations:

$$\rho^2 t' = aD + \frac{(r^2 + a^2)P}{\Delta} \tag{1.20a}$$

$$\rho^4 r'^2 = \Delta(qr^2 - K) + P^2 \tag{1.20b}$$

$$\rho^4 \theta'^2 = K + qa^2\cos^2\theta - \frac{D^2}{\sin^2\theta} \tag{1.20c}$$

$$\rho^2 \phi' = \frac{D}{\sin^2\theta} + \frac{aP}{\Delta} \tag{1.20d}$$

where

$$P = (r^2 + a^2)E - La \tag{1.21}$$

$$D = L - Ea\sin^2\theta \tag{1.22}$$

and the constants E, L and K are related to the initial values of (t', r', θ', ϕ') by:

$$E = -\left(g_{tt}t' + g_{t\phi}\phi'\right) \tag{1.23}$$

$$L = g_{t\phi}t' + g_{\phi\phi}\phi' \tag{1.24}$$

$$K = \rho^4\theta'^2 - qa^2\cos^2\theta + \frac{D^2}{\sin^2\theta} \tag{1.25}$$

We now have the equations to solve. Chapter 2 will describe the scenario in which we will solve these equations as well as the methods used.

1.3 The Robertson-Walker Metric

The paradigm of modern cosmology is the Friedmann-Lemaître-Robertson-Walker (FLRW) model (Friedmann, 1922; Lemaître, 1931; Robertson, 1935; Walker, 1936). The Robertson-Walker (RW) metric, which tells us how to measure distance and time in a homogeneous and isotropic universe, has the line element:

$$\mathrm{d}s^2 = -\mathrm{d}t^2 + R^2(t)\left(\mathrm{d}\chi^2 + S_k^2\left(\mathrm{d}\theta^2 + \sin^2\theta\mathrm{d}\phi^2\right)\right) \tag{1.26}$$

where $S_k(\chi) = \sin\chi, \chi, \sinh\chi$ for $k = +1, 0, -1$, where k is the curvature constant for closed, flat and open space respectively. The RW metric relates the spacetime interval $\mathrm{d}s$ to the cosmic time t and the spherical comoving coordinates (χ, θ, ϕ). More will be said about these coordinates later. The scale factor $R(t)$ is the key prediction of any cosmological model, encapsulating the beginning, evolution and fate of the universe[4]. We can also define the Hubble parameter H, which measures the rate of expansion of the universe:

$$H \equiv \frac{1}{R}\frac{\mathrm{d}R}{\mathrm{d}t} \tag{1.27}$$

In the curved, expanding spacetime of the RW metric, we must be very careful when defining distance measures (see Linder (1997) for details and Hogg (1999) for a summary). We will use proper distance r_p, which is defined as being the radial ($\mathrm{d}\theta = \mathrm{d}\phi = 0$) spacetime interval ($\mathrm{d}s$) along a hypersurface of constant cosmic time ($\mathrm{d}t = 0$)[5]. The RW metric then gives the proper distance between the origin ($\chi = 0$) and χ at time t to be:

$$r_\mathrm{p}(t) = R(t)\chi(t) \tag{1.28}$$

The field equations of GR allow us to calculate $R(t)$ given the energy content of the universe. The result is the Friedmann equations, which, following Hobson et al. (2005), equation 15.13, we will write as:

$$H^2 = H_0^2 \sum_i \Omega_{i,0}\left(\frac{R}{R_0}\right)^{-3(1+w_i)} \tag{1.29}$$

The other two Friedmann equations can be found in Hobson et al. (2005), but will not be needed here. A subscript zero always refers to a quantity evaluated at the present epoch. The sum is over the energy components of the universe (labelled i), each with corresponding equation of state $w_i = p_i/\rho_i$, where p is the pressure and ρ is the energy density. Equation (1.29) assumes that the energy components do not interact and that each w_i is a constant[6], as it is for most familiar forms of energy—matter ($w_m = 0$), radiation ($w_r = 1/3$), vacuum energy ($w_\Lambda = -1$). The sum includes "curvature energy" ($\Omega_{k,0} = -k/(R_0H_0)^2 = 1 - \sum_{i\neq k}\Omega_{i,0}$) which has $w_k = -1/3$. This can be thought of as convenient shorthand. A particular solution to the Friedmann equations which will prove useful in Section 4.2 is the case of a universe with a single component $w > -1$:

$$R(t) = R_0\left(\frac{t}{t_0}\right)^{\frac{2}{3(1+w)}} \tag{1.30}$$

where t_0 is the age of the universe. For $w = -1$, we have the solution $R(t) = R_0\exp\left(\frac{t-t_0}{t_0}\right)$, where t_0 is the e-folding time for the expansion. We will not consider phantom energy with $w < -1$ (see Caldwell et al., 2003, and references therein for details).

[4] not to be confused with the Ricci scalar, which will only appear in Equation (1.1) in this report.

[5] A thought experiment for measuring proper distance is as follows: we imagine being at one end of a giant ruler, pointed at a distant object. A volunteer is sent along the ruler to read off the distance to the object. Since the universe is expanding, the volunteer will need to carry a clock that displays cosmic time, and note down the time when the measurement was made. When light rays have carried the volunteer's result back to us, we will know the proper distance to the object at the time the measurement was made. Samuel (2005) criticises proper distance as "violating the principle that instantaneous non-local measurements cannot be made". This amounts to criticising a spacelike interval for being a spacelike interval. In any GR metric, length or distance is defined as the spacetime interval along a surface of constant time, and as such can never be known instantaneously. This does not mean, however, that proper distance is unphysical. It only means that it must be reconstructed at a later time from the information in light signals.

[6] Evolving equations of state and interacting components will only be considered with regards to their asymptotic behaviour—cf. footnote 1; see Barnes et al. (2005) and references therein for details on such cosmological models.

The trajectory of a particle in the universe is computed by solving the geodesic equations (1.6). For the RW metric, we have

$$g_{ab} = \text{diag}(-1, R^2, R^2 S_k^2(\chi), R^2 S_k^2(\chi) \sin^2\theta) \tag{1.31}$$

which gives:

$$t'' + R\dot{R}\left(\chi'^2 + S_k^2(\chi)\left(\theta'^2 + \sin^2\theta\phi'^2\right)\right) = 0 \tag{1.32a}$$

$$\chi'' + 2Ht'\chi' - S_k(\chi)C_k(\chi)\left(\theta'^2 + \sin^2\theta\phi'^2\right) = 0 \tag{1.32b}$$

$$\theta'' + 2Ht'\theta' + 2\frac{C_k(\chi)}{S_k(\chi)}\chi'\theta' - \sin\theta\cos\theta\phi'^2 = 0 \tag{1.32c}$$

$$\phi'' + 2Ht'\phi' + 2\frac{C_k(\chi)}{S_k(\chi)}\chi'\phi' + 2\cot\theta\phi'\theta' = 0 \tag{1.32d}$$

$$-t'^2 + R^2\left(\chi'^2 + S_k^2(\chi)\left(\theta'^2 + \sin^2\theta\phi'^2\right)\right) = q \tag{1.32e}$$

where a prime means $\mathrm{d}/\mathrm{d}\lambda$, and an overdot means $\mathrm{d}/\mathrm{d}t$. $C_k(\chi) = \mathrm{d}S_k(\chi)/\mathrm{d}\chi = \cos\chi, 1, \cosh\chi$ for $k = +1, 0, -1$. Equation (1.32e) is the normalisation condition for the four-velocity (1.9). In this report, we will only consider timelike geodesics ($q = -1$), for reasons detailed later.

Equations (1.32a)-(1.32d) allow a trivial solution, i.e. χ, θ, ϕ = constant for all time. Thus, there exists a family of free-falling particles that maintain their position in comoving coordinates—in fact, this is what we mean by comoving coordinates. This family of particles defines the Hubble flow.

For motion in one dimension, we can exploit the isotropy and homogeneity of the metric to choose our coordinates to make the motion purely radial. Gron & Elgaroy (2006) study this case and derive the following useful equations:

$$\dot{\chi} = (R^2 + CR^4)^{-1/2} \tag{1.33a}$$

$$\chi = \chi_0 \pm \int \frac{\mathrm{d}t}{R\sqrt{1 + CR^2}} \tag{1.33b}$$

where

$$C = \frac{1}{\dot{\chi}_0^2 R_0^4} - \frac{1}{R_0^2} \tag{1.34}$$

is strictly positive. Note that these are equations for χ as a function of t not λ.

Chapter 3 will describe the scenario in which we will solve these equations as well as the methods used.

Chapter 2

Looking at Kerr Black Holes

In Chapter 1, we wrote down the equations (1.20) that describe the motion of freely falling particles in Kerr spacetime. The question now arises: in what particular situation should we solve these equations? What paths should we consider (timelike, null or spacelike), and how should we set their initial conditions?

Rather than trying to solve for every possible particle path, we will focus here on a scenario with astrophysical applications. The modern astrophysical theory of Active Galactic Nuclei (AGN) states that these extremely luminous objects associated with galaxies are powered by a central supermassive ($M \sim 10^9 M_{sun}$) black hole and accretion disk. The formation of the black hole and accretion disk out of collapsing, rotating matter will result in a Kerr black hole and a thin accretion disk located in the equatorial plane.

An interesting question to ask is: what would the accretion disk look like if we could see it? What distortions would the black hole create in our view of the accretion disk? It is this specific question that we will answer in this chapter. The geometry of the situation is illustrated in Figure 2.1. We consider light particles emitted from a certain position in the disk and travelling away from the black hole toward a "CCD camera" located a large distance away (so that spacetime can be considered approximately Minkowskian). Each "pixel" on the image then stores the location of the emitter in the accretion disk, and can be coloured appropriately.

In fact, we can make our job easier by noting that the paths of the photons are time reversible. Thus we can "emit" the photons from the CCD and trace their path toward the accretion disk. This saves us following photons from the accretion disk away from the black hole only to find that they miss our camera.

The algorithm for creating an image of an accretion disk around a black hole is as follows:

1. Choose the parameters for the black hole M and a. In our chosen units, M merely sets the length scale so we can normalise it to $M = 1$, unless we want Minkowski spacetime ($M = 0$). This

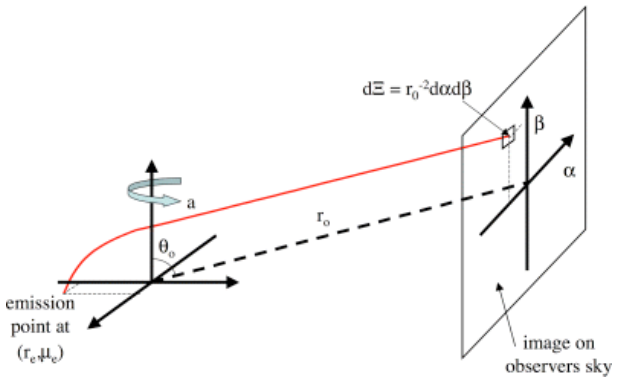

Figure 2.1: The geometry of the accretion disk and CCD. Image taken from Beckwith & Done (2004) — note that they have used r_o and θ_o for our r_{obs} and θ_{obs}, and that $\mu_e = \cos\phi$. Also labeled is the infinitesimal solid angle element dΞ.

means that we measure distances in units of gravitational radii ($r_g = GM/c^2$) and that $0 \leq a \leq 1$. We also set $q = 0$ for photons following null geodesics.

2. Choose the inner r_{in} and outer r_{out} radii of the accretion disk. We will set the inner radius to be slightly greater than the innermost stable circular orbit (for a co-rotating disk): $r_{in} = 1.5r_{ms}$. We choose the outer radius so that the distortions close to the black hole are apparent, since these are the most physically interesting. We chose $r_{out} = 5r_{ms}$.

3. Choose the position of the centre of the CCD $(r_{obs}, \theta_{obs}, \phi_{obs})$. The value of ϕ_{obs} is arbitrary owing to azimuthal symmetry. The value of r_{obs} would be chosen to be infinity in an analytic treatment, but since we will be using numerical integrators it is set to be large enough that space is approximately flat but not too large that our integration path is unnecessarily long. We choose $r_{obs} = 10^3$ (having tested against larger values and found negligible change). The orientation angle θ_{obs} has physical significance, and so we run the code for a range of values.

4. Choose the number of pixels (n) on each side of the CCD, for a total of n^2 pixels. This parameter more than any other determines the time taken to execute the code. We choose n to be even for the following reason: with the coordinates on the CCD as shown in 2.1, if there were an odd number of pixels, then photons would be sent on a path that would encounter the coordinate singularity on the axis of rotation. This is best avoided.

5. Choose the size of the CCD. This sets the initial coordinates of the photons. If it is set too small, the image will not fit on the CCD; if it is too large then a large fraction of pixels will "miss" the accretion disk, affecting the efficiency of the code. In general, the CCD will be approximately the same size as the disk.

6. Having fixed the size of the CCD, we evenly space the n^2 photons over the CCD, giving the initial positions of each of the photons. We begin by specifying (α, β) in the coordinate system of the CCD. We can then use basic geometry to transform into the black hole coordinates (by assuming that we are sufficiently removed from the black hole to treat space as Euclidean. The relevant equations can be found in Book (2004).

7. We now need to set the initial 4-velocity of the photons, or equivalently, set their constants of motion. All photons begin propagating perpendicular to the CCD. The equations relating (α, β) to (E, L, K) are derived in Chandrasekhar (1983, pg. 347). In fact, the trajectory of photons does not depend on their energy E, so we can set $E = 1$:

$$L = \alpha E \sin\theta_{obs} \tag{2.1}$$

$$K = \beta^2 - a^2\cos^2\theta_{obs} + \frac{L^2}{\tan^2\theta_{obs}} + (L - aE)^2 \tag{2.2}$$

8. For each photon, integrate the equations of motion (1.20), sending the photon towards the black hole. We now need to know when to stop. In short, keep going until: a) it hits the equatorial plane (between r_{in} and r_{out}); b) it hits the black hole (using the criteria discussed in Section 2.2); or c) it misses everything and is moving away from the accretion disk again. In each case, record the result (in particular, r and ϕ if it hits the disk) and move on to the next photon[1].

2.1 The Inside-Out Algorithm

In above algorithm, we spend a lot of time integrating geodesics that miss everthing. In fact, these are the iterations that take the most time, as we have to integrate until the photon is well clear of the accretion disk. We could save ourselves some time by changing the size of the CCD so that the edges of the picture

[1]We consider a geometrically thin but optically thick disk. In particular, we exclude the possibility of photons passing through the disk.

are as close to pixels that hit the edge of the accretion disk as possible. This depends on both r_{out} and θ_{obs}, so it is tricky to predict ahead of doing the actual integration.

I had another idea. The photons that miss the disk are usually around the outside of the image. So if, for a given pixel, all the other pixels between it and the centre of the image are "misses", then the given pixel is a "miss" too. However, if we cycle through the pixels row-and-column wise, then we don't know whether the pixels inside a given pixel miss or not, since they haven't been calculated yet.

The idea is simple — we rearrange the order of the pixels so that they are numbered from the inside-out. Then for each pixel, we know the fate of all the particles inside that pixel (viewing the array as being comprised of rectangular "shells" of pixels). Before we begin integrating the photon path, we test to see whether it is outside pixels that we know miss the black hole. If it is, we move on to the next pixel, saving a significant amount of time.

We can illustrate the details of the procedure as follows. For a 6 by 6 pixel image, the order by which the pixels would be cycled through row-and-column wise is:

$$\begin{array}{cccccc} 1 & 2 & 3 & 4 & 5 & 6 \\ 7 & 8 & 9 & 10 & 11 & 12 \\ 13 & 14 & 15 & 16 & 17 & 18 \\ 19 & 20 & 21 & 22 & 23 & 24 \\ 25 & 26 & 27 & 28 & 29 & 30 \\ 31 & 32 & 33 & 34 & 35 & 36 \end{array} \tag{2.3}$$

Before integrating pixel 6, we would like to know whether or not pixels 9, 10, 11, 17 and 23 miss the black hole, but they haven't been calculated yet. Instead, we rearrange the order of the pixels:

$$\begin{array}{cccccc} 17 & 18 & 19 & 20 & 21 & 22 \\ 36 & 5 & 6 & 7 & 8 & 23 \\ 35 & 16 & 1 & 2 & 9 & 24 \\ 34 & 15 & 4 & 3 & 10 & 25 \\ 33 & 14 & 13 & 12 & 11 & 26 \\ 32 & 31 & 30 & 29 & 28 & 27 \end{array} \tag{2.4}$$

Now, before we begin integrating the photon from pixel 22, we can check to see whether pixels 6, 7, 8, 9 and 10 all miss the accretion disk. If they all do, we record that pixel 22 missed the disk and move on to pixel 23. In this way, we do not waste time on photons that do not contribute to the final image[2].

2.2 Individual Photons

The next step in developing a code that implements this algorithm is the last step — write and test a code that integrates the geodesic equations for a single photon. The code requires a numerical ODE solver — we use the adaptive Runge-Kutta routine in Press et al. (1992). The implementation of Equations (1.20) is relatively straightforward, but for the problems encountered by photons that fall into the black hole.

To fully overcome the event horizon singularity, we need to change our coordinates. This would allow us to follow the path of the photon through the event horizon and toward the ring singularity. However, here we are not interested in the path of photons once they are inside the black hole. It is enough to know that a photon will enter the black hole. The photon sphere defines the relevant cut-off — a photon at r_c must have zero radial velocity to maintain an orbit around the black hole. Thus, if a photon crosses r_c from the outside, it has a negative radial velocity ($r' < 0$) and will not escape the black hole. However, as we noted in the introduction, for an extreme kerr black hole $r_c = r_+$ i.e. the photon sphere and the event horizon coincide. As a result we use the policy that the integrator will stop when the photon is within 1% of the photon sphere.

[2]A few minor details: the code actually tests 7 pixels, not 5 i.e. for pixel 22, test pixels 5, 6, 7, 8, 9, 10 and 11. Also, when implementing the tests, we must split the array into 4 quadrants and write different code for each. For pixels near the boundaries between the quadrants (e.g. 19 or 34 above), we test pixels in a line rather than an 'L' shape. For example, for pixel 34, test pixels 5, 16, 15, 14 and 31.

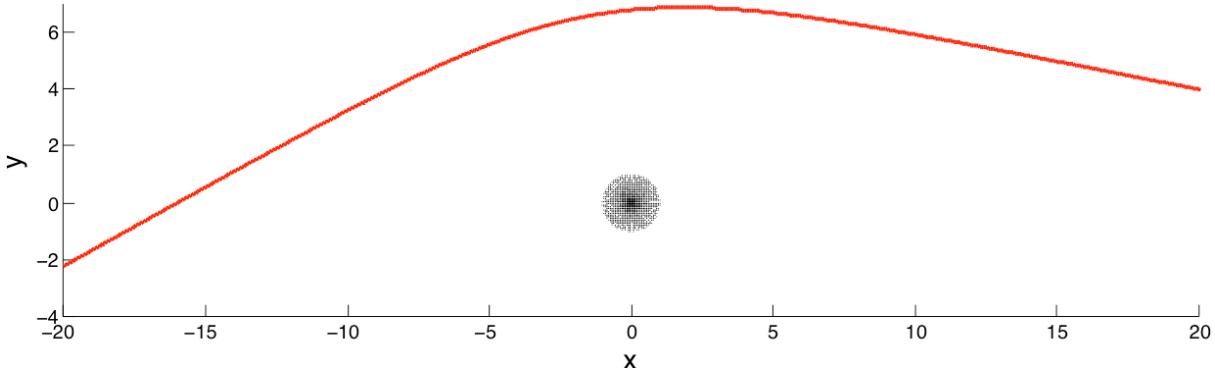

Figure 2.2: The path of a photon passing close to the black hole but not falling in.

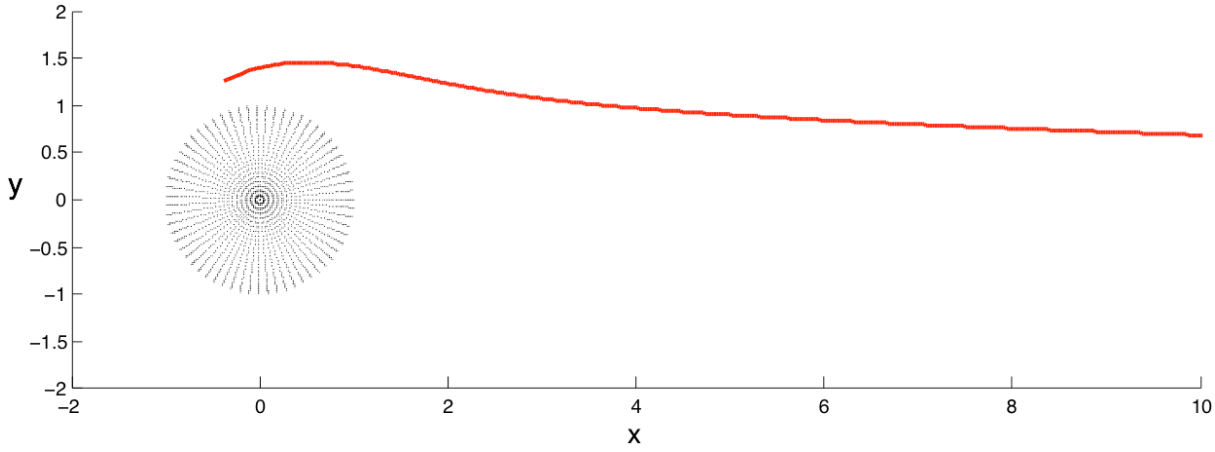

Figure 2.3: The path of a photon falling into the black hole. Note that the path stops short of the black hole, as we cannot numerically integrate up to the event horizon. Note also that the photon doesn't fall 'straight in' — it is swept in an anti-clockwise direction by the rotational effects of the black hole on the surrounding spacetime (i.e. frame-dragging).

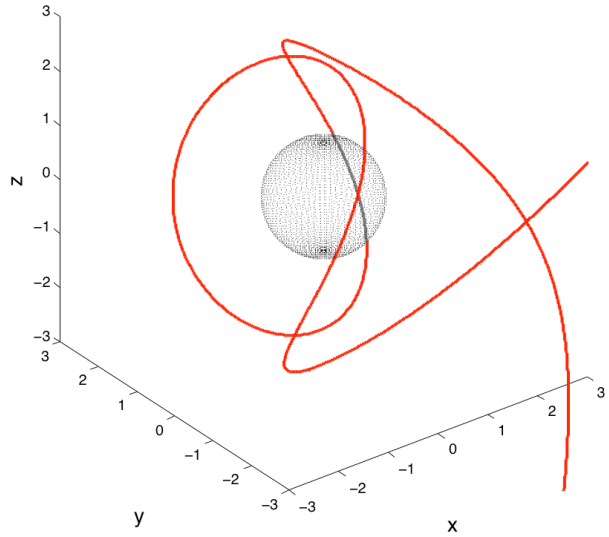

Figure 2.4: An extreme example of a photon whose path is altered by the black hole. The grey portion of the path passes behind the black hole.

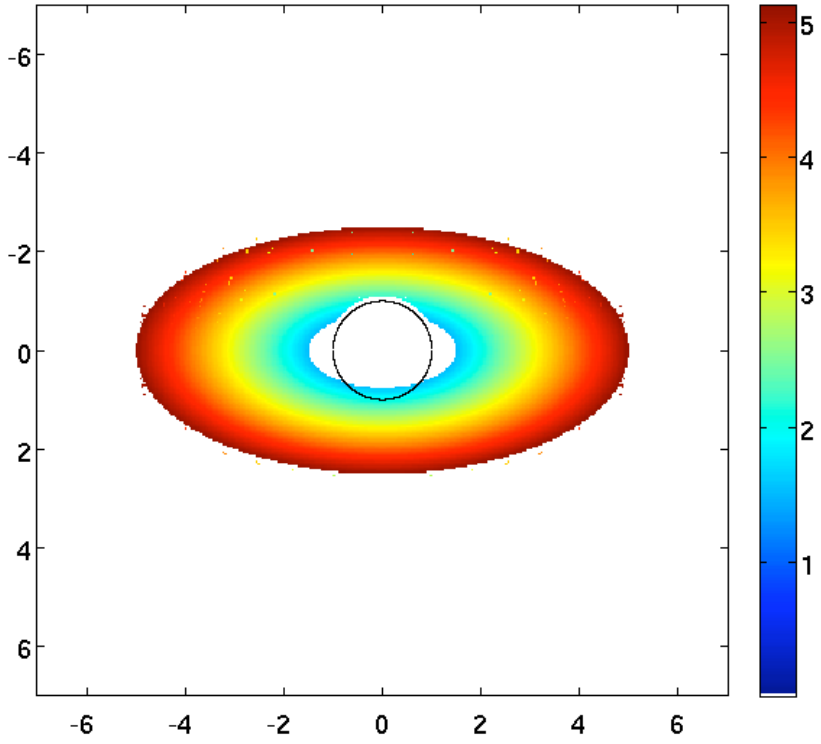

Figure 2.5: An image of the disk with no black hole present, viewed at an inclination of $\theta_{obs} = \pi/3$. The legend to the right of the image shows the colour scheme used to indicate the radial coordinate r of the point on the disk. The black ring shows the outline of where the black hole would be.

Figures 2.2 - 2.4 show some example paths. In all figures, $a = 1$ and the axis of rotation of the black hole is the z-axis The grey circle/sphere shows the outer event horizon. Figure 2.2 shows the trajectory of a photon whose path is bent as it passes close to the black hole. Figure 2.3 shows a photon falling into the black hole. This particular path (with $\theta' = 0$, known as a principal null path) has an analytic solution D'Inverno (1992, pg. 257) that was used to check the accuracy of the numerical integrator. Figure 2.4 shows an extreme example of a photon whose path is significantly altered by the black hole.

2.3 Accretion Disks

We can now implement the full algorithm and create an image of the accretion disk. The two physical parameters we need to alter are the angular momentum a and the inclination angle θ_{obs}. We begin by showing an image of the disk in flat spacetime i.e. with no black hole and thus no light bending. Figure 2.5 shows an disk inclined at an angle of $\theta_{obs} = \pi/3$ in Minkowski spacetime ($M = 0$, $a = 0$). We colour the pixels of the image according to their radial coordinate r, as shown in the legend of Figure 2.5.

2.3.1 Changing the Angular Momentum (a)

The effect of changing the angular momentum a is shown in Figure 2.6. We set the angle of inclination to $\theta_{obs} = \pi/3$ and colour the disk according to radial coordinate as before. Recall that the inner and outer radii of the disk (r_{in} and r_{out}) depend on r_{ms} and thus depend on a.

The distortion of the disk relative to the flat spacetime case (Figure 2.5) is very obvious. Two effects are very noticeable. The first is the distortion of the far side of the disk. The reason for this is easy to identify—photons from the CCD which would ordinarily pass over the top of the disk are bent down onto the disk by the attraction of the black hole. As a result, the back of the disk appears to be bent

upwards. The second effect is the secondary image of the disk, below the upper primary one. This image results from photons passing under the front of the disk whose paths then curve upwards to collide with the underside of the far side of the disk.

Slightly less obvious is the effect of changing a. The case $a = 0$ is Schwarzschild spacetime and shows the expected symmetry about the vertical axis. As we increase a, an asymmetry forms as photons from one side of the disk are swept along by the frame-dragging effects of the rotation of the black hole, while photons from the other side of the disk are propagating against the flow.

2.3.2 Changing the Angle of Inclination (θ_{obs})

The effect of changing the angle of inclination θ_{obs} is shown in Figure 2.7. We set the angular momentum to $a = 1$ and, as before, colour the disk according to radial coordinate. The most striking of these images is for $\theta_{obs} = \pi/2$. With no black hole, this image would be blank as we are looking edge on at a geometrically thin disk. The presence of the black hole means that photons passing above and below the front of the disk are bent onto the top and underside of the far side of the disk respectively. Thus this image, in spite of its similarity with the $\theta_{obs} = 0$ image, is in fact two views of the far side of the disk.

2.4 Redshift and Blueshift

We can colour the disk more meaningfully by colouring according to the redshift or blueshift measured for a photon emitted from the relevant point on the disk. Conceptually, there are two contributions to this change in frequency: a redshift due to the fact that the photon must climb out of the potential well of the black hole (the gravitational redshift), and a shift due to the motion of the emitter relative to the observer (the Doppler shift). Before we can calculate the Doppler shift, we need to know the velocity of each point on the disk. In a Newtonian model, we would assign circular, Kepler orbits to each particle in the disk, so that their velocity is related to their radius by:

$$v = \sqrt{\frac{GM}{r}} \tag{2.5}$$

However, we are so close to the black hole that a Newtonian model is likely to be inaccurate. We instead use the equations for a timelike, circular ($r' = 0$) geodesic orbit that is co-rotating with the black hole, as found in Hobson et al. (2005). We can summarise the relevant equations as follows: the energy of a particle with 4-momentum p^μ measured by an observer with 4-velocity u^μ is:

$$E = -u^\mu p_\mu = -g_{\mu\nu} u^\mu p^\nu \tag{2.6}$$

The observer, a long way from the black hole, has constant spatial coordinates so their 4-velocity is: $u_0^\mu = (1, 0, 0, 0)$. Thus, the observed energy E_{obs} is:

$$E_{obs} = -p_0 \tag{2.7}$$

Meanwhile, for the emitter in the disk: $u^2 = \theta' = 0$, since the particle is confined to the equatorial plane, and $u^1 = r' = 0$, since the particle is in a circular orbit. Thus, the 4-velocity of the emitter is given by $u^\mu = (t', 0, 0, \phi')$. Both t' and ϕ' are calculated in Hobson et al. (2005, Equation 13.40), where the constants h and k appearing in those equations are calculated for the case of circular orbits in Equation 13.54 and 13.55 of Hobson et al. (2005). The emitted energy E_e is then:

$$E_e = -(t' p_0 + \phi' p_3) \tag{2.8}$$

The calculation of p_0 and p_3 is simplified by two facts: firstly, the absence of t and ϕ in the metric tensor means that p^0 and p^3 are conserved, meaning that we need only calculate them at one end of the photon trajectory; and secondly, these quantities are calculated when we integrate the geodesic equations along the particle path, and are thus readily available in the code.

The result is shown in Figure 2.8. We use the parameters $a = 1$ and $\theta_{obs} = \pi/3$, and colour the pixels various shades of red or blue depending on the ratio of the observed frequency to the emitted frequency.

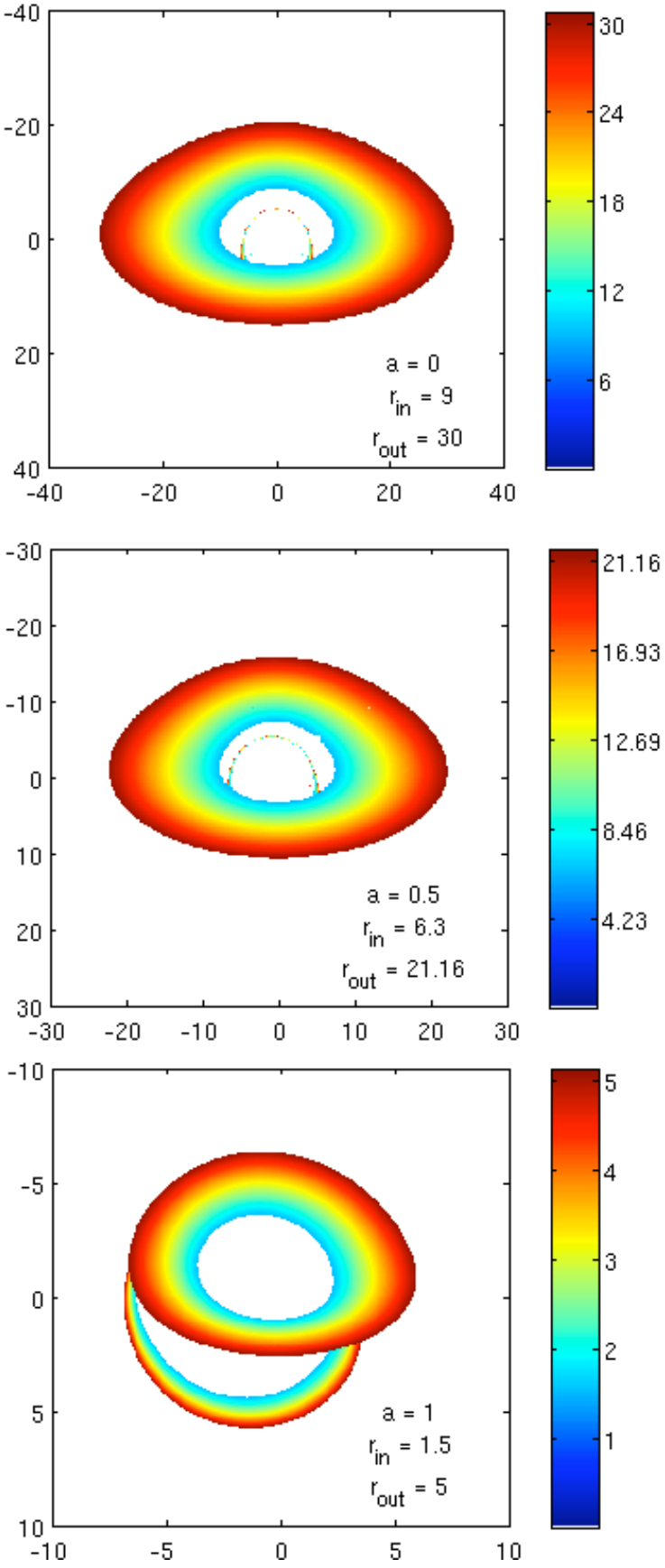

Figure 2.6: Images of the disk with varying values of a, as shown in each plot. The angle of inclination is $\theta_{obs} = \pi/3$ and we colour the disk according to radial coordinate as in Figure 2.5.

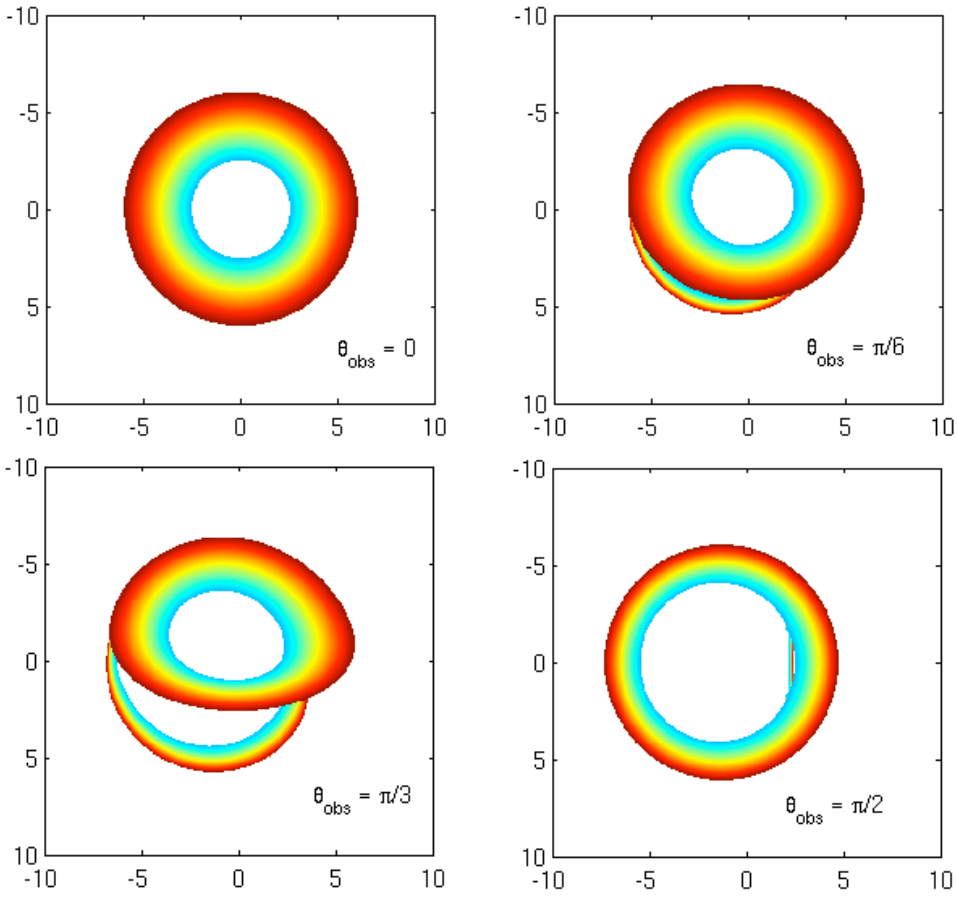

Figure 2.7: Images of the disk with varying values of θ_{obs}, as shown in each plot. The angular momentum is $a = 1$ and we colour the disk according to radial coordinate as in Figure 2.5. The vertical lines in the interior of the $\theta_{obs} = \pi/2$ plot are from photons that encircle the black hole and encounter the other side of the disk.

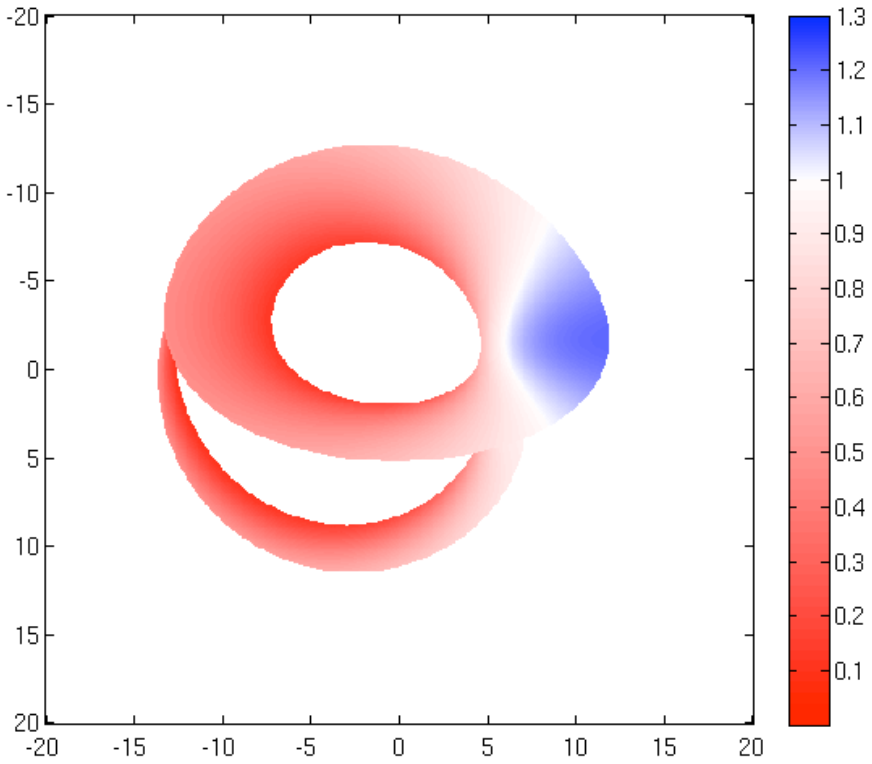

Figure 2.8: An image of the disk coloured according to the ratio of the observed to the emitted frequency. We use the parameters $a = 1$ and $\theta_{obs} = \pi/3$. The legend to the right shows the value of the ratio of the observed frequency to the emitted frequency.

We can see that, for the side of the disk where the emitter velocity is toward the observer, the Doppler blueshift is more significant than the gravitational redshift, resulting in a net blueshift. There is a white band in Figure 2.8 that shows the region where Doppler blueshift and gravitational redshift are exactly opposed. The rest of the disk has a net redshift, increasing toward the centre where the gravitational well is deepest.

We have compared our results with similar investigations in the literature. We find good qualitatively agreement with Bromley et al. (1997); Fanton et al. (1997); Beckwith & Done (2004, 2005): the back of the disk appears to bent upwards, with a similar pattern of redshift and blueshift from different parts of the disk. Quantitatively, simulations were run to allow a direct comparison with Figure 1 of Bromley et al. (1997) using the parameters: $a = 1$; $r_{in} = 1.25$; $r_{out} = 10$; $\theta_{obs} = 75°$. Excellent agreement was found between the two simulations.

It is worth noting that accretion disks in AGN are too small to be imaged by current telescopes, so the images shown previously cannot be checked observationally. However, the ray tracing codes can be used to predict the spectral line profile of line emission from the disk; see Bromley et al. (1997); Fanton et al. (1997); Beckwith & Done (2004, 2005). The codes I have developed will be used to this end

2.5 Spherical Coronae

Many models of AGN include, along with an accretion disk in the equatorial plane, a hot corona located above and below the disk. These are often associated with highly ionised iron lines in the spectra of AGN (see,amongst others Haardt & Maraschi, 1993; Dove et al., 1997). As a toy model to illustrate the appearance of an object surrounding the black hole, we can consider an image of a sphere at a radius r_{sph}.

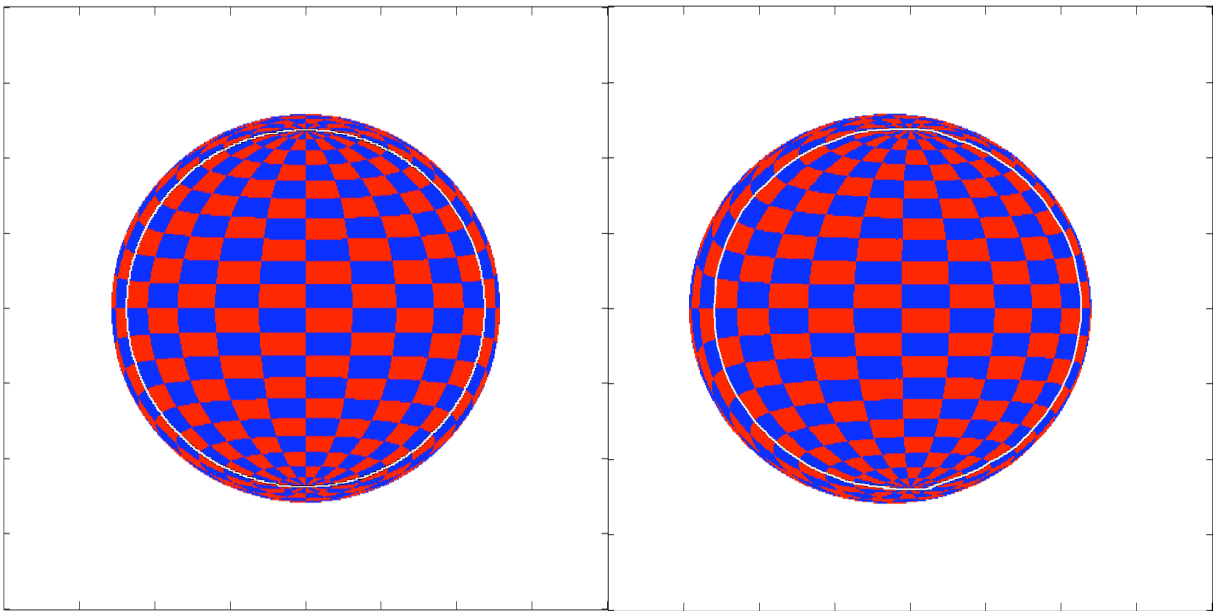

Figure 2.9: Images of a spherical corona surrounding a black hole. The angle of inclination is $\theta_{obs} = \pi/2$, the radius of the sphere is $r_{sph} = 5M$ and the value of a is shown in each panel. We have tiled the surface of the sphere with alternating colours: there are 20 panels along a line of longitude, and 20 panels around a line of latitude. The light line inside each image shows the great cirlce corresponding to the limit of what could be seen by an observer infinitely far away in flat spacetime. In other words, anything in the image that is outside the light line is "around the back" of the sphere.

The changes to the code from previous sections are minimal, as we need only change the stopping conditions (i.e. the final step of the algorithm given at the start of this chapter). We integrate the path of the photon until it passes inside r_{sph}, where we record the azimuthal (ϕ) and polar (θ) angle of impact before moving onto the next photon. The inside-out algorithm is again useful.

The result is shown in Figure 2.9. We set the angle of inclination to $\theta_{obs} = \pi/2$, and consider the two cases of a Schwarzschild black hole ($a = 0$), and an extreme Kerr black hole ($a = 1$). For both images, we have set $r_{sph} = 5M$ to allow easier comparison of the two cases. To show the varying values of ϕ and θ, we have tiled the surface of the sphere with alternating colours, as explained in the caption.

In both cases, we see that the bending of light allows us to see around the back of the sphere. This is most obviously seen at the top and bottom of the image, where we can see the north and south pole. It can also been seen at the sides of the sphere, where we can see more than the 10 panels that would be visible if the black hole were not present.

Chapter 3

Motion of Test Particles in Robertson-Walker Spacetime

In recent years there has been debate over paradoxical features of the FLRW model, and the physical interpretation of its dynamics. Attention has been drawn in particular to superluminal recession velocities (Davis & Lineweaver, 2001; Davis et al., 2003; Chodorowski, 2006; Sitnikov, 2006) and to the motion of test particles in expanding space (Davis et al., 2003; Whiting, 2004; Gron & Elgaroy, 2006; Peacock, 2006). It is to the second of these issues that we turn our attention.

The motion of test particles in the FLRW model is a fascinating illustration of the interaction between physical concepts and quantitative theories. One of the defining characteristics of physics is the mathematical precision of its predictions. Yet there is more to applying physical laws than simply solving equations. In order to make physical laws more transparent and accessible, we use physical concepts that develop an intuition or a mental picture of the scenario. A successful physical concept allows us to shortcut the mathematics, qualitatively understanding a scenario without having to solve the equations. As an example, consider the north pole of a bar magnet approaching a loop of wire. Looking from behind the magnet, we know that an anti-clockwise current will be set up in the wire, but we need not come to this conclusion by solving Maxwell's equations—Lenz's law will give us the answer without the mathematics.

Attached to the equations of the FLRW model is the physical concept that "space is expanding". Galaxies, we are taught, are receding not because they are moving through space but because space itself is being stretched between us and the galaxy. On the face of it, this concept gives us a good intuitive understanding of many cosmological phenomena—it helps us understand why the velocity-distance law is linear and why light is redshifted as it moves through the universe. However, it has been attacked recently, most notably by Whiting (2004) and Peacock (2006), as being inadequate in describing local dynamics. Whilst Peacock (2006) will allow a global form of the expanding space concept—the total volume of a closed universe increases with time—he contends that:

> there is no local effect on particle dynamics from the global expansion of the universe ... 'Expanding space' is in general a dangerously flawed way of thinking about an expanding universe.

Previous attempts at resolving this debate have suffered from a number of shortcomings. The most common is the overwhelming desire to approximate General Relativity (GR) by something else—Newtonian gravity, Special Relativity (SR) or a weak field limit of GR. This is probably wrong and certainly unnecessary—why approximate when you can use the exact geodesic equations? Another problem is the small range of cosmological models considered—Gron & Elgaroy (2006), for example, do a marvellous job of solving the geodesic equations and then apply the solution to just two models, both of which are observationally disfavoured. There is also a dangerous reliance on numerical calculations to determine asymptotic ($t \to \infty$) behaviour. Whiting (2004) makes this point about Davis et al. (2003), but doesn't say why analytic solutions to a Newtonian approximation are better than numerical solutions of the exact GR equations. Most importantly, there are hidden assumptions about what expanding space does and does not mean. We will address these problems in this and following chapters.

Following previous work on this topic, we set up the initial conditions of our test particle as follows. We place ourselves at the origin ($\chi = 0$) and the test particle at χ_0. We consider the particle to initially have constant proper distance $\dot{r}_{\rm p}(t_0) = 0$ i.e.

$$\frac{\mathrm{d}\left(R(t)\chi\right)}{\mathrm{d}t}\Big|_{t=t_0} = 0 \quad \Rightarrow \quad \dot{R}(t_0)\chi_0 + R(t_0)\dot{\chi}(t_0) = 0 \tag{3.1}$$

The reason for this particular initial condition is quite simple. A popular way of visualising expanding space is a balloon or a large rubber sheet. Imagine yourself and a friend at rest on a large rubber sheet. We cannot directly observe spacetime, so we will do this thought experiment in the dark[1]. Suppose you both observe a glowing ball moving away from you. "The rubber sheet is being stretched," you say. "No it's not," replies your friend, "the sheet is still and the ball is rolling away." Together, you come up with an ingenious way of finding out who is right. You take another glowing ball, and drop it onto the sheet a certain distance away. If the sheet is expanding, then we expect it to carry the ball away; if the sheet is still then the recession of the first ball was due to a kinematical initial condition. Once this is removed, so is the recession.

The cosmological expansion is a bit more complicated, as we have expansion that changes with time due to the self gravitation of the energy contents of the universe. We will therefore need to consider a range of cosmological models. For reasons that will become clear in the next section, we will consider models given by Equation (1.30). We will allow χ to be negative when a particle passes through the origin, rather than have to worry about a change in angular coordinates. We have chosen $t_0 = 1$ and $R_0 = 1$ for each model. We started each particle off at comoving coordinate $\chi_0 = 1/3$, which ensures that $C > 0$. Physically, this ensures that we do not place the particle beyond the Hubble sphere, which would require a velocity relative to the local Hubble flow (peculiar velocity) greater than the speed of light[2].

The results of solving the geodesic equations numerically are shown in Figure 3.1. The dotted line in the centre panels shows the motion of the particle as calculated by a Newtonian analysis (see Whiting (2004) and Peacock (2006)). The equation of motion is:

$$r_{\rm p}^{\rm Newton} = 2R_0\chi_0\left(\frac{t}{t_0}\right)^{1/3} - R_0\chi_0\left(\frac{t}{t_0}\right)^{2/3} \tag{3.2}$$

The Newtonian result is surprisingly accurate, remaining close to the GR solution even up to 100 times the age of the universe. It is seen to diverge from the exact solution eventually, though, and thus remains only a useful approximation for small times. This divergence becomes more apparent as we increase χ_0, i.e. as we approach the Hubble sphere. If we consider the $w = 0$, Einstein de-Sitter universe and set $\chi_0 = 1$, then the solutions diverge much more quickly. Figure 3.2 reproduces Figure 1 of Whiting (2004), overlaying the relativistic solution. It is easy to see that whilst the qualitative behaviour is similar, the Newtonian solution is quantitatively different.

Returning to Figure 3.1, a few points are noteworthy. The bottom, leftmost panel ($w = -2/3$) shows the particle trajectory moving away from the origin and very quickly becoming indistinguishable from the nearby Hubble flow. The other panels do not show the same behaviour, but instead the particle moves toward the origin and away on the opposite side of the sky. Moreover, they don't seem to be attaching themselves to any particular particle in the Hubble flow. But, as noted in the introduction, it is dangerous to try to determine asymptotic behaviour from numerical plots. We must do it analytically.

[1] We will not speculate on how you two came to be standing on a rubber sheet in the dark.

[2] Gron & Elgaroy (2006), equation (22) gives this condition incorrectly. The correct formula, which follows directly from their equation (21), is $\chi_0 < 3(1+w)/2$. They then claim to start at particle off at $\chi_0 = 1$ in a Milne ($w = -1/3$) universe, which contradicts the previous condition on χ_0. Therefore, their Figure 1b) appears to plot a null geodesic.

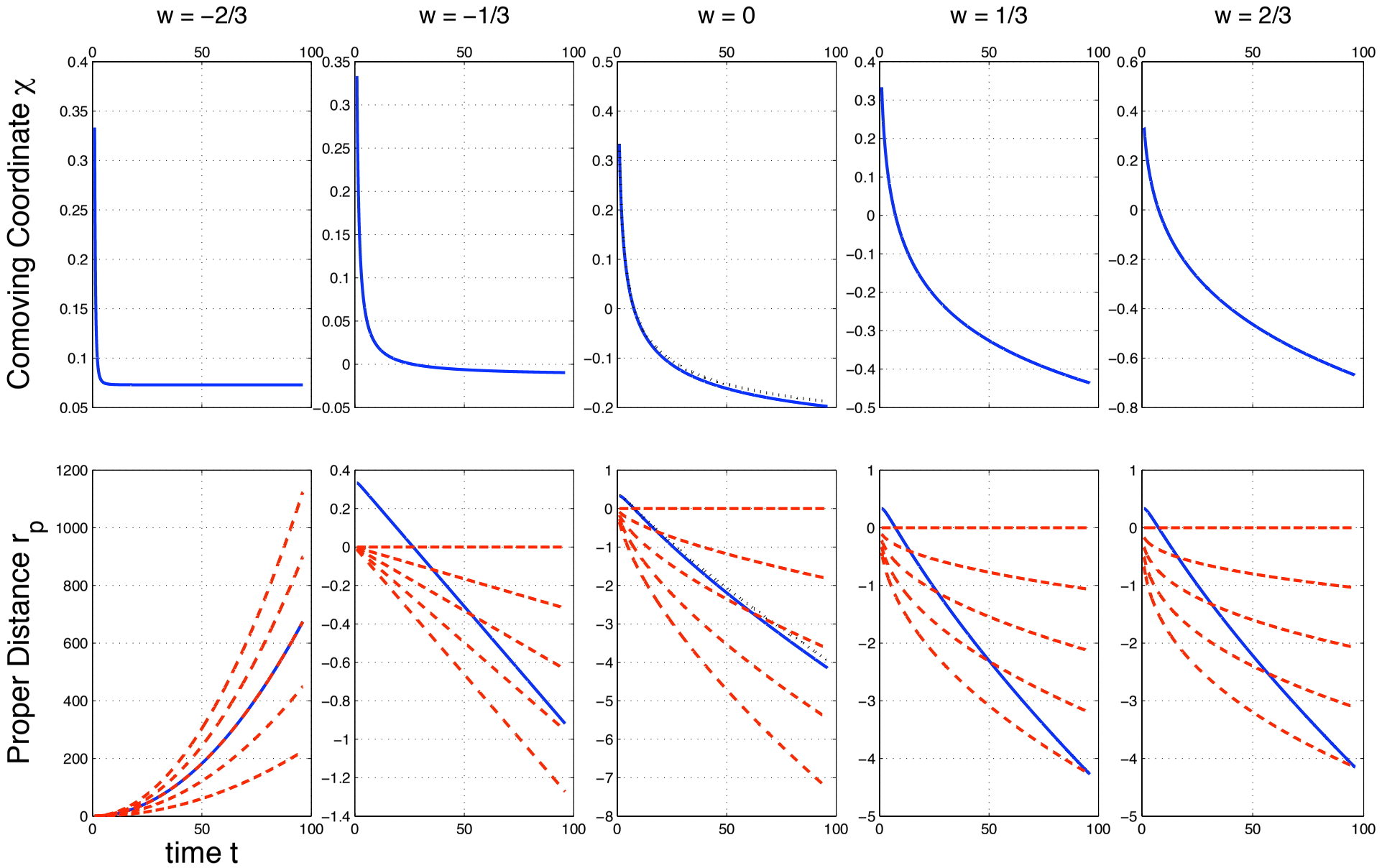

Figure 3.1: Comoving radial coordinate and proper distance (solid lines) as a function of time for a particle in radial motion for cosmological models with differing values of the equation of state w given above each column. The dashed lines in the lower panels show the motion of nearby particles in the Hubble flow. The dotted line in the centre panels gives the Newtonian solution for the motion of the particle, as discussed in the text. Note that the vertical scale changes from panel to panel.

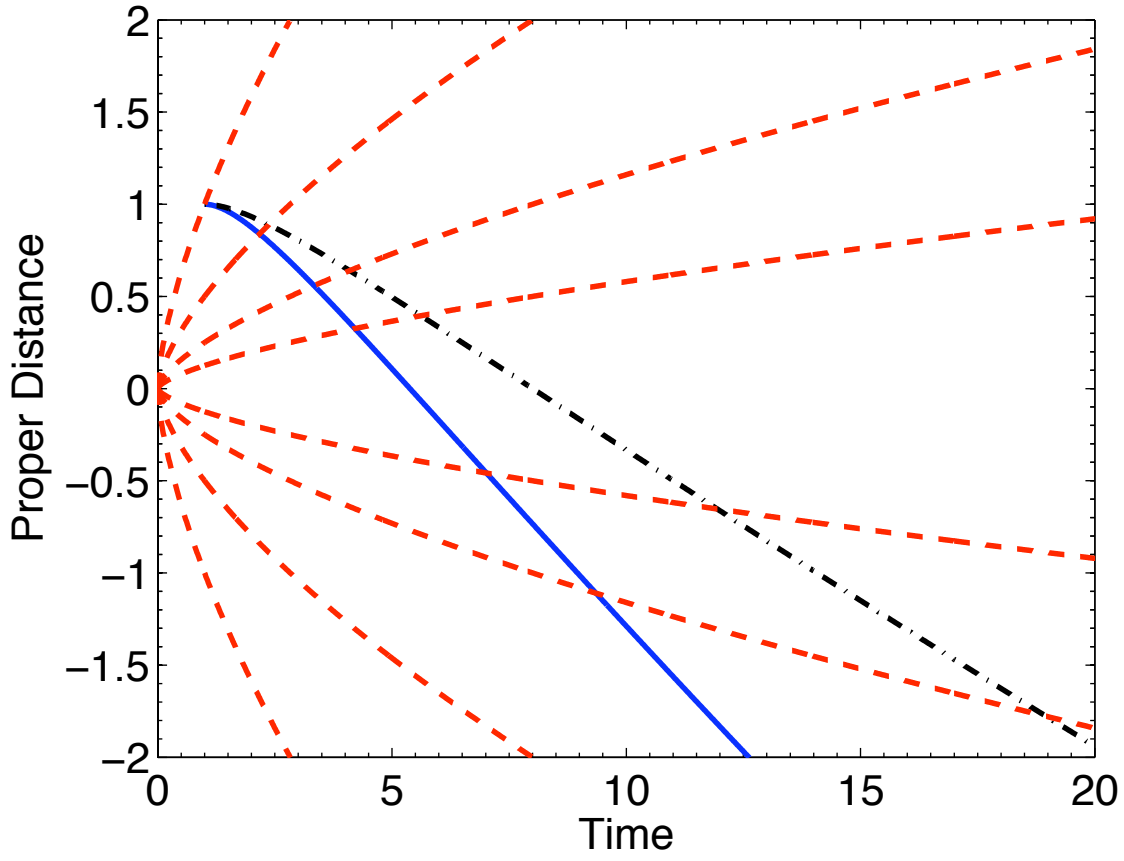

Figure 3.2: A reproduction of Figure 1 in Whiting (2004), plotting proper distance against time for a test particle released from $\chi_0 = 1$ in an Einstein de-Sitter universe (i.e. flat, matter only). The dot-dashed line is the Newtonian solution, whilst the solid line is the relativistic solution. The dashed lines represent particles in the Hubble flow. The discrepancy between the solutions is obvious.

Chapter 4

Joining the Hubble Flow

There is disagreement in the literature as to the fate of free particles in an eternally expanding universe, i.e. where $R(t) \to \infty$ as $t \to \infty$. Davis et al. (2003) and Gron & Elgaroy (2006) claim that they will asymptotically rejoin the Hubble flow, whilst Whiting (2004) states that "it cannot be asserted that ... free particles [are] swept into the Hubble flow, even asymptotically." This is an important issue because it is often claimed that the expansion of space will dampen out all motion through space, so that a particle initially removed from the Hubble flow will asymptotically rejoin it.

On closer inspection, this disagreement stems from different definitions of what it means to "asymptotically rejoin the Hubble flow." In this section we will propose a number of precise definitions of this phrase, and then see which ones are equivalent and which ones hold in an eternally expanding but otherwise arbitrary universe. We will not consider universes in which the current expansion becomes a contraction at some point in the future. This would be an unnecessary and distracting complication when considering the expansion of space. We do not claim that this list is exhaustive.

4.1 Seven Definitions

Definition 1 ($\dot{\chi} \to 0$): A particle with coordinate trajectory $\chi(t)$ asymptotically rejoins the Hubble flow if $\dot{\chi}(t) \to 0$ as $t \to \infty$.

The particle is deemed to asymptotically rejoin the Hubble flow if its velocity through coordinate space approaches the velocity through coordinate space of the Hubble flow, namely zero.

Definition 2 ($\chi \to \chi_\infty$): A particle with coordinate trajectory $\chi(t)$ asymptotically rejoins the Hubble flow if $\chi \to \chi_\infty$ as $t \to \infty$, where χ_∞ is a constant that depends on the cosmology and initial conditions.

The Hubble flow is defined by having constant coordinates. Thus, we consider a particle to approach the Hubble flow if its radial coordinate approaches a constant. The asymptotic value of the radial coordinate (χ_∞) can be thought of as the "rightful place" of the particle in the Hubble flow.

Definition 3 ($v_{\mathbf{pec}} \to 0$): A particle with coordinate trajectory $\chi(t)$ asymptotically rejoins the Hubble flow if $v_{\mathbf{pec}}(t) \equiv R(t)\dot{\chi}(t) \to 0$ as $t \to \infty$.

We can divide the proper velocity ($\dot{r}_{\rm p}$) of a test particle into a recession component and a peculiar component as follows:

$$\dot{r}_{\rm p} = \dot{R}(t)\chi(t) + R(t)\dot{\chi}(t) = v_{\rm rec}(t) + v_{\rm pec}(t) \tag{4.1}$$

If we move our coordinate origin so that $\chi(t) = 0$ at time t, then we see that the proper velocity of the test particle is solely its peculiar velocity. Thus peculiar velocity is simply proper velocity relative to the local Hubble flow. The requirement that $v_{\rm pec}(t) \to 0$ as $t \to \infty$ is equivalent to the velocity relative to the local Hubble flow going to zero.

Definition 4 ($\dot{r}_{\mathbf{p}} \to v_{\mathbf{rec}}$): A particle with coordinate trajectory $\chi(t)$ asymptotically rejoins the Hubble flow if $\dot{r}_{\mathbf{p}} \to v_{\mathbf{rec}}(t)$ as $t \to \infty$.

We require that the proper velocity of the test particle approaches its recession velocity. This is subtly different from definition 3, as will be explained below. To avoid ambiguity, this definition uses a continuous version of asymptotic equivalence: we say that $f(x)$ approaches $g(x)$ as $x \to \infty$ if their ratio approaches unity, i.e.

$$f(x) \to g(x) \text{ as } x \to \infty \quad \Leftrightarrow \quad \frac{f(x)}{g(x)} \to 1 \text{ as } x \to \infty \tag{4.2}$$

Definition 5 ($\Delta r_{\mathbf{p}} \to 0$): A particle with coordinate trajectory $\chi(t)$, where $\chi(t) \to \chi_\infty$ as $t \to \infty$, asymptotically rejoins the Hubble flow if $\Delta r_{\mathbf{p}} \equiv |R(t)\chi_\infty - R(t)\chi(t)| \to 0$ as $t \to \infty$.

Suppose that our test particle is approaching a particular coordinate ($\chi = \chi_\infty$, cf. definition 2) and that we place a reference particle in the Hubble flow at this coordinate. We require that the proper distance between the test particle and the reference particle approach zero. In other words, the test particle sees its rightful place in the Hubble flow get closer (in terms of proper distance) asymptotically. Note that if we had chosen instead to require that $R(t)\chi(t) \to R(t)\chi_\infty$ then this definition would have been equivalent to Definition 2 by Equation (4.2).

Definition 6 ($z_{\mathbf{obs}} \to z_{\mathbf{cosm}}$): A particle with observed redshift $z_{\mathbf{obs}}(t_r)$ at time of reception t_r asymptotically rejoins the Hubble flow if $z_{\mathbf{obs}}(t_r) \to z_{\mathbf{cosm}}$ as $t_r \to \infty$, where t_e is the time of emission of a photon that reaches the observer at t_r.

Light emitted from a particle in the Hubble flow is observed to be redshifted according to the cosmological redshift formula: $z_{\text{cosm}} \equiv R(t_r)/R(t_e) - 1$. For a particle with coordinate trajectory $\chi(t)$, there is an additional Doppler redshift resulting from its velocity relative to the Hubble flow:

$$1 + z_{\text{obs}}(t_r) = (1 + z_{\text{cosm}})(1 + z_{\text{Dop}}) \tag{4.3}$$

$$= \left(\frac{R(t_r)}{R(t_e)}\right)\left(\frac{1 + v_{\text{pec}}(t_e)}{1 - v_{\text{pec}}(t_e)}\right)^{\frac{1}{2}} \tag{4.4}$$

where v_{pec} is considered positive when the particle's velocity through the local Hubble flow points away from us. The Doppler term is the familiar redshift of light formula from SR, but the formula is derived purely from the RW metric.

This definition assumes that we are comoving observers that measure light signals sent from the test particle. Suppose at each time we place a reference particle in the Hubble flow at the same coordinate as the test particle. The redshift of the reference particle, which represents the local Hubble flow, will be purely cosmological. This definition requires that the redshift of the test particle approach the redshift of the reference particle.

Definition 7 (CMB dipole $\to 0$): A particle moving through a universe containing a cosmic microwave background (CMB) asymptotically rejoins the Hubble flow if the dipole anisotropy in the CMB goes to zero as $t \to \infty$.

In a universe filled with black-body radiation at a certain temperature T, an observer moving through the Hubble flow will see the CMB to be hotter in one direction and colder in the opposite direction. Indeed, this is exactly what we see from Earth—it is known as the "great cosine in the sky" and disrupts the isotropy of the CMB at a level of $\sim 10^{-3}$ (Bennett et al., 2003, among others). The maximum difference between the temperature as measured by an observer in the Hubble flow (T_0) and our test particle with peculiar velocity $v_{\text{pec}} << c$ is given by (Peebles & Wilkinson, 1968; Melchiorri et al., 2002):

$$\frac{\Delta T}{T_0} \sim \frac{v_{\text{pec}}}{c}. \tag{4.5}$$

Finally, note that it is too much to ask that the test particle exactly join the Hubble flow after some time, i.e. $\chi(t) = \chi_{\rm f}$, a constant, for all $t \geq t_{\rm f}$. Only pathological functions that do not equal their own Taylor series can do this, and it is unlikely that such functions will appear as a solution to the geodesic equations (1.32).

4.2 Comparing the Definitions

The previous section may appear to be an exercise in pedantic cosmology, and one hopes that all the definitions will turn out to be equivalent. However, it turns out that only three of the above definitions hold in eternally expanding but otherwise arbitrary universes, and one of them fails in all non-accelerating universes.

We will need two key results in order to analyse these definitions. The first is that all eternally expanding cosmological models approach the single component model of Equation (1.30) as $t \to \infty$. We can show this directly from Equation (1.29). Consider the universe to contain a number of energy components (labelled i), each with constant[1] equation of state w_i. Now consider the right hand side of Equation (1.29). As $t \to \infty$, we know that $R(t) \to \infty$ since we are only considering eternally expanding universes. Since the dependence on $R(t)$ is $R^{-3(1+w_i)}$, we see that, for large t, the component with the most negative equation of state will dominate the dynamics of the universe. Precisely, let the component with the most negative equation of state be called the dominant component ($i = d$), with equation of state w_d. Then, for large t

$$H^2 \approx H_0^2 \, \Omega_{d,0} \left(\frac{R}{R_0} \right)^{-3(1+w_d)} \tag{4.6}$$

$$\Rightarrow \quad R(t) \approx R_0 \left(\frac{t}{t_0} \right)^{\frac{2}{3(1+w_d)}} \tag{4.7}$$

which is Equation (1.30) with $w = w_d$. For example, in a universe with matter density less than critical, we consider "curvature energy" to be the dominant component with $w_d = -1/3$. The exact solution for this cosmology (given in Hobson et al. (2005), pg. 402) indeed shows that $R(t) \propto t$ for large t. Thus, Equation (4.7) is a general form for $R(t)$ when considering the asymptotic behaviour of the universe[2]. We can also calculate the deceleration parameter, q:

$$q \equiv -\frac{\ddot{R}}{R} \frac{1}{H^2} = \frac{1}{2}(3w_d + 1) \tag{4.8}$$

Thus, if $w_d > -1/3$ then the expansion of universe will decelerate; if $w_d < -1/3$, then the universe will eventually accelerate; if $w_d = -1/3$ then the universe will approach a coasting universe.

The second key result is the asymptotic behaviour of the integral for χ in Equation (1.33b) when $R(t)$ given by Equation (4.7). Whilst the exact indefinite integral unfortunately involves the hypergeometric function, we can approximate this function in the limit of large t as by noting that $\sqrt{1 + CR^2} \approx \sqrt{C}R$ in this limit. The integral then becomes trivial. We now analyse the seven definitions, in order from the weakest to the strongest conditions.

Definition 1 ($\dot{\chi} \to 0$): From Equation (1.33b) we can see that as $t \to \infty$ (and $R(t) \to \infty$), $\dot{\chi} \propto R^{-2}$. Thus Definition 1 holds in all eternally expanding universes, so that the velocity of a particle through coordinate space will always decay to zero. Gron & Elgaroy (2006) use this definition when they claim that test particles will rejoin the Hubble flow.

[1] For a component with an evolving equation of state, consider the asymptotic value of the equation of state, i.e. $w_i(t) \to w_{i,\infty}$ as $t \to \infty$. A unbounded equation of state is most likely unphysical. An oscillating equation of state will not be considered.

[2] There is a subtlety here—a universe that contains only "curvature energy" (i.e. an empty universe) is not identical to a universe containing a critical density fluid with equation of state $w = -1/3$. Although the dependence of the scale factor on time is the same in both universes ($R(t) \propto t$), the empty universe has $k = -1$, whilst the $w = -1/3$ fluid universe has $k = 0$. However, Equations (1.32) show that if we consider radial geodesics ($\theta' = \phi' = 0$), then there is no dependence on k. Thus, the distinction between these two universes can be ignored for now.

Definition 3 ($v_{\text{pec}} \to 0$): Since $v_{\text{pec}}(t) = R(t)\dot{\chi}(t)$, Definition 3 is stronger than Definition 1. However, it still holds in all eternally expanding universes, since Equation (1.33b) shows that as $t \to \infty$, $v_{\text{pec}}(t) \propto R^{-1}$. This is closely related to the well known result that the momentum of any particle in the universe decays as R^{-1}. It is this definition that is most widely used to justify the claim that test particles rejoin the Hubble flow asymptotically.

Definition 7 (CMB dipole $\to 0$): Equation (4.5) shows that this definition is equivalent to Definition 3 and thus holds in all eternally expanding universes. In particular, this shows that the dipole in the CMB will decay faster than the CMB temperature itself.

Definition 2 ($\chi \to \chi_\infty$): At first sight, Definition 2 may appear to be a direct consequence of Definition 1—surely if the derivative of a function approaches zero then the function itself will approach a constant. However, it is easy to think of counterexamples: $f(x) = \log(x)$. Thus, we need to consider Equation (1.33b), integrating between $t_0 = 1$ and t and using the two approximations discussed at the start of this section. This gives:

$$\chi(t) = \chi_0 \pm \int_1^t \frac{\mathrm{d}t}{R\sqrt{1 + CR^2}} \tag{4.9}$$

$$\approx K_1 \pm \frac{1}{\sqrt{C}R_0^2} \int^t \frac{\mathrm{d}t}{t^{2n}} \tag{4.10}$$

where $n = \frac{2}{3(1+w_d)}$ and K_1 is a constant that includes χ_0 and the primitive of the exact integral evaluated at t_0. Thus, for the integral to be bounded as $t \to \infty$, we require that:

$$2n > 1 \quad \Rightarrow \quad w_d < 1/3 \tag{4.11}$$

Thus if we use Definition 2 to define what it means to asymptotically rejoin the Hubble flow, then test particles in universes where the dominant energy component has equation of state $w_d \geq 1/3$ do not rejoin the Hubble flow. In particular, in a universe where the dominant energy component is radiation, the comoving coordinate of a test particle removed from the Hubble flow increases (or decreases) without bound. The particle has no rightful place in the Hubble flow[3].

Definition 4 ($\dot{r}_{\text{p}} \to v_{\text{rec}}$): Definition 4 appears to be identical to Definition 3; surely if $\dot{r}_{\text{p}}(t) = v_{\text{rec}}(t) + v_{\text{pec}}(t)$ and $v_{\text{pec}}(t) \to 0$ in all eternally expanding universes then Definition 4 holds trivially. However, it is possible that $v_{\text{rec}}(t)$ also goes to zero, and if it does so as fast or faster than $v_{\text{pec}}(t)$ then we are not justified in saying that the proper velocity of the test particle approaches its recession velocity. We can see this from Equation (4.2):

$$\dot{r}_{\text{p}}(t) \to v_{\text{rec}}(t) \quad \Rightarrow \quad \frac{\dot{r}_{\text{p}}(t)}{v_{\text{rec}}(t)} \to 1 \tag{4.12}$$

$$\Rightarrow \quad \frac{v_{\text{rec}}(t) + v_{\text{pec}}(t)}{v_{\text{rec}}(t)} \to 1 \tag{4.13}$$

$$\Rightarrow \quad \frac{v_{\text{pec}}(t)}{v_{\text{rec}}(t)} \to 0 \tag{4.14}$$

which is stronger than the condition in Definition 3. Whiting (2004, p. 11) hinted at Definition 4: "Peculiar velocities do vanish eventually in expanding universes; but so do *all* velocities [emphasis original]", but mistakenly implied that it would rule out rejoining the Hubble flow in matter dominated universes ($w_d = 0$). Davis et al. (2003) use Definition 4 (see their equation (11) and following) but mistakenly believe that it follows automatically from the success of Definition 3.

As we noted previously, as $t \to \infty$, $v_{\text{pec}}(t) \propto R^{-1}$. Thus:

$$v_{\text{pec}}(t) \propto R^{-1} \propto t^{-n} \tag{4.15}$$

[3]Hartle (2003) sets the derivation of Equation (1.33b) as a practice problem for undergraduates. The solutions give a very instructive derivation using Killing vectors, but then state that the particle comes to rest at coordinate $x_f \equiv \chi_\infty$, given by integrating from zero to infinity. He fails to note that the integral may diverge, so that the particle may not come to rest at all.

We now consider $v_{\text{rec}}(t) = \dot{R}(t)\chi(t)$. Using Equation (4.10) we approximate χ by:

$$\chi(t) \approx K_1 \pm \frac{1}{\sqrt{C}R_0^2} \begin{cases} \frac{t^{1-2n}}{1-2n} & \text{if } n \neq 1/2 \\ \log t & \text{if } n = 1/2 \end{cases} \tag{4.16}$$

$$\Rightarrow \quad v_{\text{rec}}(t) \propto K_2 t^{n-1} + K_3 \begin{cases} t^{-n} & \text{if } n \neq 1/2 \\ t^{-1/2}\log t & \text{if } n = 1/2 \end{cases} \tag{4.17}$$

where the K_i will be used keep track of constants. Now, we need to consider three cases:

- If $n > 1/2$, then $n - 1 > -n$. Thus the dominant term in Equation (4.17) is the first term so that $v_{\text{rec}}(t) \propto t^{n-1}$ for large t. Then, as $t \to \infty$:

$$\frac{v_{\text{pec}}(t)}{v_{\text{rec}}(t)} \propto \frac{t^{-n}}{t^{n-1}} \to 0 \tag{4.18}$$

  Thus when $n > 1/2$, $v_{\text{pec}}(t)$ goes to zero faster than $v_{\text{rec}}(t)$, meaning that Definition 4 holds.

- If $n = 1/2$, then $v_{\text{rec}}(t) \propto t^{-1/2}\log t$. Then, as $t \to \infty$:

$$\frac{v_{\text{pec}}(t)}{v_{\text{rec}}(t)} \propto \frac{t^{-1/2}}{t^{-1/2}\log t} \to 0 \tag{4.19}$$

  Thus Definition 4 holds when $n = 1/2$.

- If $n < 1/2$, then $n - 1 < -n$ so that $v_{\text{rec}}(t) \propto t^{-n}$. Then, as $t \to \infty$:

$$\frac{v_{\text{pec}}(t)}{v_{\text{rec}}(t)} \propto \frac{t^{-n}}{t^{-n}} \to 1 \tag{4.20}$$

  Thus when $n < 1/2$, $v_{\text{rec}}(t)$ and $v_{\text{pec}}(t)$ approach zero at the same rate. It is not true that $\dot{r}_{\text{p}}(t) \to v_{\text{rec}}(t)$ as $t \to \infty$ and Definition 4 fails in this case.

If we use Definition 4 to define what it means to asymptotically rejoin the Hubble flow, then test particles in universes where the dominant energy component has equation of state $w_d > 1/3$ do not rejoin the Hubble flow. Note that Definition 4 holds in a universe where the dominant energy component is radiation, unlike Definition 2, which fails.

Definition 6 ($z_{\text{obs}} \to z_{\text{cosm}}$): Once again we are tempted to assume that the success of Definition 3 will ensure that this definition will hold in all universes. The argument proceeds as before: if

$$1 + z_{\text{Dop}} = \left(\frac{1 + v_{\text{pec}}(t_e)}{1 - v_{\text{pec}}(t_e)}\right)^{\frac{1}{2}} \tag{4.21}$$

and $v_{\text{pec}}(t) \to 0$ in all eternally expanding universes then Definition 6 holds trivially. And our *caveat* is the same—we must be careful of the case where z_{cosm} also goes to zero.

To do this, we need to express z_{obs} in terms of reception time t_r and then consider the limit $t_r \to \infty$. In fact it is much easier to express everything in terms of the emission time t_e and then consider $t_e \to \infty$; $t_e < t_r$ guarantees that both cases will have identical limiting behaviour.

In the limit of small v_{pec}, we have that $z_{\text{Dop}} \sim v_{\text{pec}} \propto t^{-n}$, using Equation (4.15). Also, $1 + z_{\text{cosm}} = \frac{R(t_r)}{R(t_e)} = \frac{t_r^n}{t_e^n}$, so that the task at hand is to express t_r in terms of t_e. Consider a light ray travelling along a null ($\mathrm{d}s = 0$), ingoing ($\mathrm{d}\chi < 0$), radial ($\mathrm{d}\theta = \mathrm{d}\phi = 0$) geodesic. From the RW metric:

$$\mathrm{d}t = -R(t)\mathrm{d}\chi \tag{4.22}$$

$$\Rightarrow \chi(t_e) - \chi(t_r) = \int_{t_e}^{t_r} \frac{\mathrm{d}t}{R(t)} \tag{4.23}$$

where we now place the receiver at the origin: $\chi(t_r) = 0$. For the case of a test particle removed from the Hubble flow, $\chi(t_e)$ is given by Equation (1.33b), approximated by Equation (4.16). An immediate

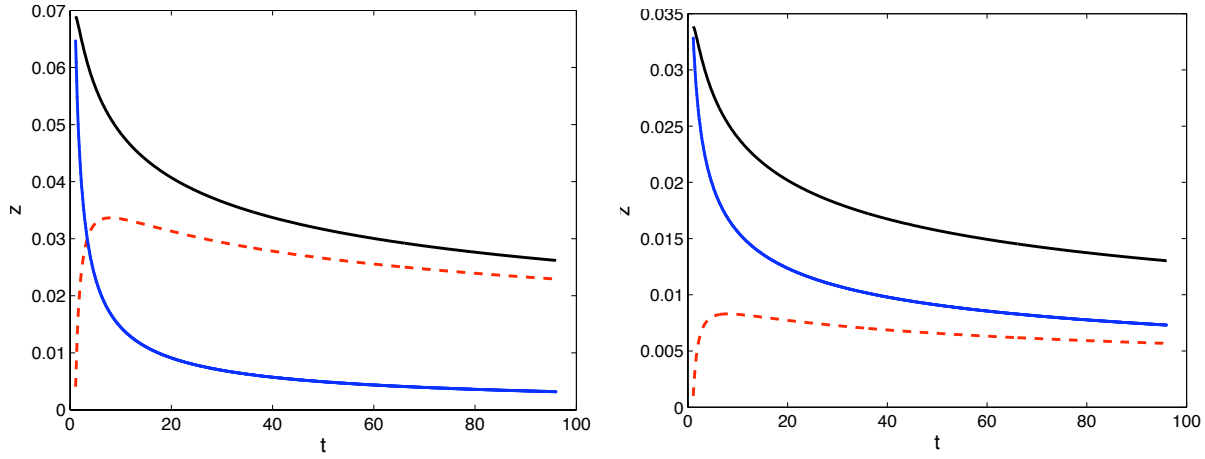

Figure 4.1: Redshift as a function of time for cosmological models with $w = 0$ (left) and $w = 1$ (right) (examples of fluids with $w = 1$ are free massless scalar fields and shear energy, such as superhorizon gravitational waves; see Linder (1997)). The red dashed line is the cosmological redshift (z_{cosm}), the blue solid line is the Doppler redshift (z_{Dop}) and the solid black line is the observed redshift ($z_{\text{obs}} = -1+(1+z_{\text{cosm}})(1+z_{\text{Dop}})$). The left panel shows the asymptotic dominance of the cosmological redshift for $w \leq 1/3$, whilst the right panel shows the identical asymptotic behaviour of the cosmological and Doppler redshift at large t for $w > 1/3$.

consequence of combining these equations is that Definition 6 must work in accelerating and coasting universes ($w_d \leq -1/3$), since in these universes z_{cosm} does not go to zero. Thus we need only consider $0 < n < 1$. We will leave the $n = 1/2$ case to the reader: it involves $\log t$ as with Definition 4.

With this in mind, we can derive an expression for t_r:

$$t_r = \left(t_e^{1-n} + K_4 t_e^{1-2n} + K_5\right)^{\frac{1}{1-n}} \tag{4.24}$$

which leads to the following expression for $1 + z_{\text{cosm}}$:

$$1 + z_{\text{cosm}} = \left(1 + K_4 t_e^{-n} + K_5 t_e^{-(1-n)}\right)^{\frac{n}{1-n}} \tag{4.25}$$

$$\approx 1 + K_6 t_e^{-n} + K_7 t_e^{-(1-n)} \tag{4.26}$$

where the last expression is calculated using the binomial theorem for non-integer exponents[4]. This leads to the following three cases:

- If $n > 1/2$, then $n - 1 > -n$ so that $z_{\text{cosm}} \propto t^{n-1}$. Then, as $t \to \infty$:

$$\frac{z_{\text{Dop}}}{z_{\text{cosm}}} \propto \frac{t^{-n}}{t^{n-1}} \to 0 \tag{4.27}$$

  Thus when $n > 1/2$, z_{Dop} goes to zero faster than z_{cosm}, meaning that Definition 6 holds.

- If $n = 1/2$, it turns out that $z_{\text{cosm}} \propto t^{-1/2} \log t$. Then, as $t \to \infty$:

$$\frac{z_{\text{Dop}}}{z_{\text{cosm}}} \propto \frac{t^{-1/2}}{t^{-1/2} \log t} \to 0 \tag{4.28}$$

  Thus Definition 4 holds when $n = 1/2$.

- If $n < 1/2$, then $n - 1 < -n$ so that $z_{\text{cosm}} \propto t^{-n}$. Then, as $t \to \infty$:

$$\frac{z_{\text{Dop}}}{z_{\text{cosm}}} \propto \frac{t^{-n}}{t^{-n}} \to 1 \tag{4.29}$$

  Thus when $n < 1/2$, z_{cosm} and z_{Dop} approach zero at the same rate. It is not true that $z_{\text{obs}} \to z_{\text{cosm}}$ and Definition 6 fails in this case.

[4] See Weisstein (2006) for a reminder.

Table 4.1: Seven definitions and the conditions for their fulfilment.

	Definition	Hold in all expanding universes?	If no, conditions on w_d for definition to hold
1	$\dot{\chi} \to 0$	yes	
2	$\chi \to \chi_\infty$	no	$w_d < 1/3$
3	$v_{\text{pec}} \to 0$	yes	
4	$\dot{r}_{\text{p}} \to v_{\text{rec}}$	no	$w_d \leq 1/3$
5	$\Delta r_{\text{p}} \to 0$	no	$w_d < -1/3$
6	$z_{\text{obs}} \to z_{\text{cosm}}$	no	$w_d \leq 1/3$
7	CMB dipole $\to 0$	yes	

If we use Definition 6 to define what it means to asymptotically rejoin the Hubble flow, then test particles in universes where the dominant energy component has equation of state $w_d > 1/3$ do not rejoin the Hubble flow. The situation is illustrated in Figure 4.1. When $w = 0$ the Doppler redshift decays away much faster than the cosmological redshift, so that Definition 6 holds. However, when $w = 1$ the Doppler and the cosmological redshift decay at the same rate; which one is greater depends on the cosmological model and the initial conditions (hidden in the constants K_i). Thus, Definition 6 fails in this universe.

Definition 5 ($\Delta r_{\text{p}} \to 0$): We know already that this definition fails in some cases since it relies on Definition 2. Thus we begin with the assumption that $w_d < 1/3$, i.e. $n > 1/2$. Now, we have that:

$$\Delta r_{\text{p}} = |R(t)\chi_\infty - R(t)\chi(t)| \tag{4.30}$$

$$= R(t)\left| \int_{t_0}^{\infty} \frac{\mathrm{d}t}{R\sqrt{1+CR^2}} - \int_{t_0}^{t} \frac{\mathrm{d}t}{R\sqrt{1+CR^2}} \right| \tag{4.31}$$

$$= R(t)\left| \int_{t}^{\infty} \frac{\mathrm{d}t}{R\sqrt{1+CR^2}} \right| \tag{4.32}$$

$$\propto t^n \left| \int_{t}^{\infty} \frac{\mathrm{d}t}{t^{2n}} \right| \tag{4.33}$$

$$\propto t^n \, t^{1-2n} = t^{1-n} \tag{4.34}$$

Hence the requirement that $\Delta r_{\text{p}} \to 0$ as $t \to \infty$ is only met for $n > 1$, i.e. $w_d < -1/3$ or $q < 0$. In particular, for a universe where the dominant component has $w_d = -1/3$, Δr_{p} approaches a constant. For example, Whiting (2004, p. 10) reaches this conclusion for an underdense, matter only universe. If we use Definition 5 to define what it means to asymptotically rejoin the Hubble flow, then test particles in universes where the dominant energy component has equation of state $w_d \geq -1/3$ do not rejoin the Hubble flow. This means that particles asymptotically rejoin the Hubble flow only in universes that eventually accelerate. Definition 5 is the strongest of the definitions, and is the one used by Whiting (2004, p. 10) to justify the claim that particles in a matter dominated universe ($w_d = 0$) do not join the Hubble flow.

The failure of this definition can be illustrated by looking again at Figure 3.1. The first column ($w = -2/3$) clearly shows a particle that satisfies Definition 5. However, in the second and third columns ($w = -1/3, 0$), in the bottom panels, the lowest dashed line is the trajectory of the particle in the Hubble flow whose comoving coordinate is equal to χ_∞, i.e. the rightful place of the particle in the Hubble flow. In the centre column, the test particle trajectory and the rightful place trajectory move apart, whilst in the second column they are separated by a constant. Thus, the particle never joins the Hubble flow in the sense of its trajectory being indistinguishable from the trajectory of a particle in the Hubble flow.

A summary of the different definitions and the conditions for their fulfilment is given in Table 4.1. In Chapter 5, we will look closely at the implications of these results and others for the physical concept of expanding space.

Chapter 5

In Defence of Expanding Space

The attack on the physical concept of expanding space has centred on the motion of test particles in the universe, as discussed in Section 3. Whiting (2004), Peacock (2006) and others claim that the failure of expanding space to adequately explain the motion of test particles means that it should be abandoned. While it is undoubtedly true that one can formulate misleading versions of the expanding space concept, we contend that there is a formulation that avoids many of the misconceptions about RW spacetime.

5.1 The Concept of Expanding Space

The cosmological fluid provides a reference frame that all observers can agree on. That is, all observers can perform an experiment to discover their velocity relative to the cosmological fluid (e.g. anisotropy in the CMB). The global inertial frame provided by the cosmological fluid is the context in which all motion can be analysed. Motion with respect to the cosmological fluid requires a multitude of specific, astrophysical causes (e.g. the motion of the Milky Way due to the Great Attractor). By contrast, the global expansion of the cosmological fluid needs only a single cause, which we look for in the initial conditions of the universe (i.e. the expansion problem cf. Peacock (1999, p. 324)). Thus we can view the cosmological fluid as the backdrop for all other motion in the universe — the reference frame of the universe. Because the cosmological fluid is expanding, and the cosmological fluid defines the reference frame of the universe, we can say (as a slogan): by expanding space we mean that the reference frame of the universe is expanding.

Central to this formulation is the idea that objects in the Hubble flow do not remain in the Hubble flow because they are dragged along by space; they remain in the Hubble flow because they are at rest in an inertial frame. Expanding space can be thought of as a manipulation of inertial frames — everyone thinks they're stationary and yet everyone is moving away from everyone else. The universe expands whilst keeping its contents in rest frames. Objects in the Hubble flow are free-falling. There is no frictional or viscous force associated with the expansion of space.

A key feature of the Hubble flow is that velocity is directly proportional to distance. This is a necessary consequence of a homogeneous and isotropic expansion (see Harrison, 2000, p. 279) and is well illustrated by an expanding balloon. We represent galaxies in the Hubble flow by buttons glued onto the balloon. This is a good analogy for the way galaxies maintain their spatial coordinates as the universe expands (i.e. they are comoving) and also the fact that galaxies themselves do not expand with the universe. However, thinking of expanding space in terms of the rest frame of the universe exposes the flaw in the balloon analogy: the glue. Buttons glued onto a balloon have no choice but to expand with the rubber of the balloon. But galaxies in the universe have a tendency to separate because their initial conditions placed them in an expanding rest frame. This reinforces the point made by Harrison (2000, p. 333) and Peacock (1999, p. 88): the universe is not expanding because spacetime is endowed with mysterious power. Objects separate now only because they have done so in the past.

The balloon analogy, like any analogy, is useful so long as we are aware of what it successfully illustrates and what constitutes pushing the analogy too far. The balloon analogy shows how a homogeneous expansion inevitably results in velocity being proportional to distance, and also gives an intuition for how

the expansion of the universe looks the same from every point in the universe. It illustrates that the universe does not expand in space; it consists of expanding space. But using the balloon analogy to visualise a mechanism like a frictional or viscous force is taking the analogy too far. It correctly demonstrates the effects of the expansion of the universe, but not the mechanism. That the analogy fails at some level is hardly surprising: we're representing 4-dimensional pseudo-Riemannian manifolds with party supplies. We can't manipulate frames like gravity can.

We are also in a good position to understand why the expansion can be thought of locally in kinematical, even Newtonian terms. We can imagine attaching a Minkowski frame to each point in the Hubble flow. The local cosmological fluid is stationary with respect to this frame. Whilst only perfectly accurate in an infinitesimally small region, the Minkowski frame can be used as an approximation for regions much smaller than the Hubble radius. The Hubble flow is then viewed as a purely kinematical phenomenon — objects recede because they have been initially given a velocity proportional to distance. This does not argue against expanding space: the equivalence principle guarantees that any free-falling observer in any GR spacetime can use SR locally. The kinematical view is often useful, but remains only a local approximation. The exception is the Milne model: in an empty universe we can make a coordinate transformation that exchanges the RW metric for the Minkowski metric (see Harrison, 2000, p. 88), effectively extending our local Minkowski frame to all spacetime. This is only possible because there is no cosmological fluid to define the rest frame of the universe. Hence the Milne model cannot be used to make general comments on the nature of the cosmological expansion (cf. Chodorowski, 2006).

We now have three tasks before us: firstly, how does this formulation of expanding space explain the basic facts of RW cosmologies? Secondly, can the results of Section 3 be understood using this formulation of expanding space, and, if not, does this force us to discard the concept completely? Finally, can we understand the failure of so many of the criteria for joining the Hubble flow in Section 4?

5.2 The Basic Facts of Expanding Space

This section will detail a number of cosmological phenomena: paragraphs 1. to 6. derive them purely from the equations, whilst the bullet points explain how they are understood in the context of expanding space.

1. Consider two objects in the Hubble flow (at the origin and χ = constant). The proper velocity of the object at χ as measured by the observer at the origin is $\dot{r}_{\mathrm{p}}(t) = \dot{R}(t)\chi = H(t)r_{\mathrm{p}}(t)$. Thus, the proper velocity of an object in the Hubble flow is proportional to its proper distance, with the constant of proportionality depending on the rate of increase of the scale factor. This is the velocity-distance law (not Hubble's law, see Harrison, 2000).

   - As mentioned previously, this is a result of the homogeneous nature of the expansion, and, as an effect of the expansion, it is illustrated by the balloon analogy. If a button on the balloon is moved away by the expansion of the balloon a certain distance in a certain time, then a button twice a far away will move twice as far. Twice the distance in the same amount of time means twice the velocity, so that velocity is proportional to distance.

2. If we consider two objects in the Hubble flow (at the origin and χ = constant), then the proper distance between them at time t_1 is $r_{\mathrm{p}}(t_1) = R(t_1)\chi$. The proper distance at a later time t_2 is $r_{\mathrm{p}}(t_2) = R(t_2)\chi$. It follows that
$$\frac{r_{\mathrm{p}}(t_2)}{r_{\mathrm{p}}(t_1)} = \frac{R(t_2)}{R(t_1)} \tag{5.1}$$
   so that the proper distance between objects in the Hubble flow increases in proportion with the scale factor.

   - This result is related to the previous one. If the balloon itself doubles in linear size, the distance between any two buttons will also double. Thus, if space expands by a certain factor, proper distances between all objects in the Hubble flow stretch by the same factor.

3. Consider a test particle moving radially with coordinate velocity $\chi(t)$. The proper velocity of the object as measured by an observer at the origin is:

$$\dot{r}_{\rm p} = \dot{R}(t)\chi(t) + R(t)\dot{\chi}(t) \tag{5.2}$$

The first term is the same as for a particle in the Hubble flow at the same comoving coordinate and depends on the rate of increase of the scale factor. It is zero for an object at the origin or in a static universe. Now, consider the second term: the time measured on a clock (τ) attached to the particle is given by the RW line element (Equation (1.26)) as

$$c^2{\rm d}\tau^2 = c^2{\rm d}t^2 - R^2(t){\rm d}\chi^2 \tag{5.3}$$

$$\Rightarrow \quad \left(\frac{{\rm d}\tau}{{\rm d}t}\right)^2 = 1 - \left(\frac{R(t)\dot{\chi}(t)}{c}\right)^2 \tag{5.4}$$

Since τ is observable it must be real (zero for a photon): $({\rm d}\tau)^2 \geq 0$ implies that $|R(t)\dot{\chi}(t)| \leq c$. Thus, the velocity of the particle due its motion relative to the Hubble flow must be less than the speed of light; its velocity due to the increase of the scale factor is not restricted in this way.

- We interpret $\dot{R}(t)\chi(t)$ as the velocity of the object due to the expansion of the space between the observer and test particle (recession velocity), and $R(t)\dot{\chi}(t)$ as the velocity of the object due to its motion through the local rest frame (peculiar velocity). As previously mentioned, we can consider attaching a Minkowski frame to each point in the Hubble flow. Then the speed of light limits the speed of an object through space. But since there is no global Minkowski inertial frame (except for in an empty universe), the relative motion of different regions of the Hubble flow sees no speed limit. Note that the kinematical view sees no difference between recession and peculiar velocities, and thus cannot explain this result. As an illustration, for light moving radially away from the origin: $v_{\rm pec} = c$, so that $\dot{r}_{\rm p} = c + H(t)r_{\rm p} > c$. An observer who insists on extending his Minkowski frame into expanding space will encounter light travelling faster than light!

4. Suppose that light is emitted from an object moving radially with coordinate velocity $\dot{\chi}(t)$. Then, an observer at the origin measures the light to have been redshifted according to Equation (4.3). The first term is the redshift of light emitted by an object in the Hubble flow at the same comoving coordinate, and the second term is identical to the redshift of light in SR due to the relative motion of inertial frames.

- The explanation of this result is quite simple, so long as we picture light as being a classical electromagnetic wave[1]. Consider redshift from an object in the Hubble flow: if two crests of the EM wave are a distance λ_e apart at emission, then the expansion of the space will mean that the wavelength of the wave at reception λ_r has been stretched in proportion with the increase of the scale factor so that: $1 + z = \lambda_r/\lambda_e = R(t_r)/R(t_e)$. If the object is moving through space, then we include an SR redshift dependent on $v_{\rm pec}$. We can also use the kinetic view of the expansion to understand why $z = v/c$ locally, and thus why Hubble's law holds ($zc = H_0 r_{\rm p}$). The closer an observed object is to the observer, the more accurate the observer's extended Minkowski frame is. Thus, for small redshifts, we expect SR formulas to hold within experimental errors.

5. Consider a normal object consisting of many particles, held together by internal forces. Suppose that the centre of the object travels along a radial geodesic $\chi_c(t)$ in RW spacetime (i.e. $\chi_c(t)$ is a

[1] We have a few reservations about this. The case of a quantum mechanical photon is more difficult to explain—how does a point-like object stretch? Allowing its wavefunction to stretch isn't much help; expanding space adds to the uncertainty in the position of the photon? In this case, it may be better to consider the effect of expanding space, not on the photon itself, but on the observers who measure the energy of the photon. The light must pass through a succession of Minkowski frames on its way through the universe, each receding from the previous one. Thus, in the expanding rest frame of the universe, we can consider the cosmological redshift to be an accumulation of infinitesimal Doppler shifts (see Peacock, 1999, pg. 87)

solution to Equations (1.32)). Suppose further that the front of the object travels along a trajectory $\chi_f(t)$ that keeps it at a constant proper distance (L) from the centre, i.e.

$$R(t)\chi_f(t) - R(t)\chi_c(t) = L \qquad \text{(a constant)} \tag{5.5}$$

$$\Rightarrow \quad \chi_f(t) = \chi_c(t) + \frac{L}{R(t)} \tag{5.6}$$

The back of the object will move along an analogous path. Then the coordinate trajectory $\chi_f(t)$ is not a geodesic of RW spacetime. The foremost particle will experience a four-force, which can be calculated by substituting Equation (5.6) into the equation of motion of a particle experiencing a four-force f^a:

$$\frac{\mathrm{d}^2 x^a}{\mathrm{d}\lambda^2} + \Gamma^a_{bc}\frac{\mathrm{d}x^b}{\mathrm{d}\lambda}\frac{\mathrm{d}x^c}{\mathrm{d}\lambda} = \frac{f^a}{m} \tag{5.7}$$

which reduces to Equation (1.6) for $f^a = 0$. The observed force in the radial direction is given by projecting f^1 onto an orthonormal basis; the final result is equation (1) of Harrison (1995) with $U(t) = -H(t)L$ for all time. In the case of L small (compared to c/H, the Hubble radius), we have that the radial force F is:

$$F = -mL\frac{\ddot{R}}{R} \tag{5.8}$$

- This result tells us how not to understand expanding space. Thinking of expanding space in terms of the provision of an expanding rest frame avoids the misconception that expanding space will mercilessly stretch everything in the universe. Expanding space does not stretch rigid rulers — how could it? It's just a trick with inertial frames. The internal, interatomic forces in rigid objects are able to maintain the object's dimensions; Dicke & Peebles (1964) (see also Carrera & Giulini, 2006) argue that EM forces do just this. Objects are held together by forces that pull their extremities through a succession of rest frames.

  The case of objects that are held together by gravitational forces is more complicated, as these would perturb the RW metric, rather than add a four force (i.e. change the left hand side of Equation (5.7) rather than the right hand side[2]). Recall that the energy in a RW universe is described as a perfect, homogeneous fluid. This can only hold on scales big enough to make galaxies look like mere particles in a fluid. Thus the applicability of the RW metric on small scales is dubious: the true metric of spacetime would be a fantastic chimera of the RW, Schwarzschild and other metrics. However, it appears that in many circumstances, we can treat these perturbations as a Newtonian gravitational force that can maintain the dimensions of a gravitationally bound system in an expanding universe. We will not pursue this further; see Cooperstock et al. (1998); Carrera & Giulini (2006) and references therein for more details.

6. Consider an object of many particles with no internal forces. It is shot away from the origin ($\chi = 0$) with speed v_0, the first particle leaving at time t_0 and the last at $t_0 + \Delta t_0$. The length of the object is $l_0 = v_0\Delta t_0$. The object travels to an observer in the Hubble flow at χ, who measures its speed relative to him (v_f) and the time of arrival of the first (t_f) and last particle ($t_f + \Delta t_f$) in order to measure its length ($l_f = v_f\Delta t_f$). Then, from Equation (1.33b):

$$\chi = \int_{t_0}^{t_f} \frac{\mathrm{d}t}{R\sqrt{1 + C_0R^2}} = \int_{t_0+\Delta t_0}^{t_f+\Delta t_f} \frac{\mathrm{d}t}{R\sqrt{1 + C_fR^2}} \tag{5.9}$$

where C_0 and C_f are calculated from the initial conditions for each particle from Equation (1.33a). If we assume that Δt_0 and Δt_f are small, then it follows that we can assume $C_0 = C_f \equiv C$ and

[2] "Wouldn't the energy in the non-gravitational forces fields holding the object together also perturb the RW metric?" Yes, they will. Although I haven't looked into this question in detail, I believe that this perturbation would be negligible. The reason is that the rest energy of the atoms in ordinary objects dominates the energy stored in their chemical bonds. Chemical bond energies are $\sim 10^5$ J/mol $\sim 10^{-19}$J/atom, while the rest energy of a proton is $m_pc^2 \sim 10^{-10}$J. Thus, the stress energy tensor will be dominated by the contribution from the rest mass energy.

then rearrange the limits of the integral to give[3]

$$\int_{t_0}^{t_0+\Delta t_0} \frac{\mathrm{d}t}{R\sqrt{1+CR^2}} = \int_{t_f}^{t_f+\Delta t_f} \frac{\mathrm{d}t}{R\sqrt{1+CR^2}} \tag{5.10}$$

$$\Rightarrow \quad \frac{\Delta t_0}{R(t_0)\sqrt{1+CR^2(t_0)}} = \frac{\Delta t_f}{R(t_f)\sqrt{1+CR^2(t_f)}} \tag{5.11}$$

Then, using Equation (1.33a) to calculate $v_f = \dot{\chi}(t_f)R(t_f)$ and substituting for C we have that

$$\frac{l_f}{l_0} = \frac{v_f \Delta t_f}{v_0 \Delta t_0} = \frac{R(t_f)}{R(t_0)} \tag{5.12}$$

Hence, the length of the object has increased in proportion with the scale factor[4].

- This result answers the question: what if an object had no internal forces, leaving it at the mercy of expanding space? This is a rather strange object — it would very quickly be disrupted by the forces of everyday life. Nevertheless, it is a useful thought experiment. The above result shows that the object, being subject only to expanding space, has been stretched in proportion with the scale factor. These are essentially cosmological tidal forces.

  Paragraphs 5 and 6 give clear, unambiguous conditions that determine whether an object will be stretched by the expansion of space. Objects will not expand with the universe when there are sufficient internal forces to maintain the dimensions of the object[5]. For example, EM radiation is not held together by EM forces. Hence there is no contradiction in saying that objects held together by EM forces do not expand whilst EM radiation does. The expansion of space is subtle but not arbitrary.

5.3 The Challenge of Particle Motion

We now turn to the issue of test particle motion. What are the central qualitative features of particle motion that expanding space needs to explain? The most surprising feature is that, in most of the models, a particle held at constant proper distance approaches the origin when released. We can calculate the conditions for approach as follows. Since we are setting the initial proper velocity to zero, whether the particle approaches or recedes depends on the initial proper acceleration ($\ddot{r}_{\mathrm{p},0}$). From Equation (1.28) it follows that

$$\ddot{r}_{\mathrm{p}} = \ddot{R}\chi + 2\dot{R}\dot{\chi} + R\ddot{\chi} \tag{5.13}$$

$$\Rightarrow \quad \ddot{r}_{\mathrm{p}} = -qRH^2\chi + H\frac{v_{\mathrm{pec}}^3}{c^2} \tag{5.14}$$

where the second equation uses Equation (4.8) and equation (11) of Gron & Elgaroy (2006). Putting in the initial conditions (Equation (3.1)), it follows that

$$\ddot{r}_{\mathrm{p},0} = -R_0 H_0^2 \chi_0 \left(q_0 + \frac{v_{\mathrm{pec},0}^2}{c^2} \right) \tag{5.15}$$

$$\Rightarrow \quad \ddot{r}_{\mathrm{p},0} < 0 \quad \text{if} \quad q_0 > -\frac{v_{\mathrm{pec},0}^2}{c^2} \tag{5.16}$$

[3]This part of the derivation is similar to the derivation of the cosmological redshift directly from the RW metric; see, among many others, Hobson et al. (2005, p. 368).

[4]We haven't seen this derivation or result anywhere in the literature, but doubt that it is original.

[5]The initial conditions are a complicating factor. For example, if we had initially placed the particles of the "no-internal-forces" object in the Hubble flow, then the object would have expanded by the result in paragraph 2. But this is trivial — there is no justification for claiming that the particles constitute a single object. On the other hand, if we considered an object whose internal forces maintain its length and then turned off all the forces, we would have recreated the scenario in Section 3. Whilst the object would eventually expand, the action of the internal forces has biased the result by initially nullifying the expansion of the universe (see Section 5.3 below). By having all particles in the object depart from the same place in the Hubble flow with the same speed, we overcome these problems.

Thus, a particle in a decelerating universe will always approach the origin.

Can this result be understood in the context of expanding space? We contend that the answer is yes. The key is to reinterpret the initial conditions of the particle. Whiting (2004) and Peacock (2006) have in mind that Equation (3.1) describes a particle dropped innocently into the universe, like the glowing ball in Section 3. It has no proper velocity and thus no prejudice—it is free to go wherever expanding space wishes to take it. This is certainly true from a kinematic, Newtonian perspective: the particle is at rest in our chosen inertial frame and approaches the origin due to the gravitational attraction of the matter between the particle and the origin. This is locally valid and even useful, but it is not how to understand the scenario from an expanding space perspective. The motion of the particle must be analysed with respect to its local rest frame provided by the Hubble flow. In this frame, we see the original observer moving at $v_{\text{rec},0}$ and the particle shot out of the local Hubble frame at $v_{\text{pec},0}$, so that the scenario resembles a race. Since their velocities are initially equal, the winner of the race is decided by how these velocities change with time. In a decelerating universe, the recession velocity of the original observer decreases, potentially handing victory to the test particle, which catches up with the observer[6].

The difference between the kinematic and expanding space interpretation is well illustrated by Figure 1 of Davis et al. (2003). Figure 1a shows the kinematic perspective — the observer and the tethered particle are at rest with respect to each other, and the gravitational attraction of the matter between them will bring them together. Figure 1b shows the scenario as seen from the local rest frame of the tethered particle, i.e. a race between the original observer and the test particle. The original observer should view the initial conditions of the test particle, not as neutral, but as a battle between motion through space and the expansion of space. The expansion of space has been momentarily nullified by the initial conditions, so we must ask how the expansion of space changes with time.

We contend that this explanation successfully incorporates test particle motion into the concept of expanding space. In particular, it shows why it is wrong to expect, on the basis of the balloon analogy, that expanding space would carry the particle away. We need to stress that expanding space is a good way of thinking about the Hubble flow but that motion through space is more subtle. The alternative is either to give up on a physical concept entirely, so that the only rationale for the cosmological facts 1. to 6. above is that "that's what the maths tells us", or to formulate a new framework into which these facts and more can be accommodated. They first option is unsavoury; the second unlikely, unless one wants to discard GR entirely and formulate cosmology using only Newtonian ideas (see Tipler, 1996).

5.4 The Challenge of the Hubble Flow

Finally, how are we to understand the failure of so many of the definitions of joining the Hubble flow in Section (4)? The first question to ask is: what does expanding space tell us about how to rejoin the Hubble flow? Given that we can picture RW spacetime as a collection of Minkowski metrics attached to every point in the expanding Hubble flow, then (Peacock, 2006)

> particle momentum in general declines ... through the accumulated Lorentz transforms required to overtake successively more distant particles that are moving with the Hubble flow.

In other words, expanding space predicts that the peculiar velocity of a test particle will approach zero as the particle tries to catch up with the receding rest frame of the universe. Thus we expect Definition 3 (along with Definitions 1 and 7, which are weaker or equivalent conditions) to hold in all eternally expanding universes. However, expanding space does not lead us to expect that Definitions 2, 4, 5 and 6 will hold. We contend that the problem is not that expanding space has mislead us, but that describing the decay of v_{pec} as joining the Hubble flow is a misnomer. The correspondence between this particular characteristic of the trajectory of the test particle and the trajectory of particles in the Hubble flow leads us to expect that all of the features of the trajectory (χ, $\dot{\chi}$, r_{p}, $\dot{r}_{\text{p}}$, v_{pec}) will approach those of the Hubble flow trajectories (respectively, $\chi = \chi_\infty$, $\dot{\chi} = 0$, $r_{\text{p}} = R(t)\chi_\infty$, $\dot{r}_{\text{p}} = v_{\text{rec}}$, $v_{\text{pec}} = 0$). But this is too much to ask from the expansion of the universe. As we have seen, many of these conditions depend on the acceleration and deceleration of the universe, rather than just its expansion.

[6]Note that a particle in an empty, unaccelerated universe will approach the origin, as can be seen in Figure 3.1, but that this is a purely relativistic effect, being proportional to $v_{\text{pec},0}^2/c^2$ (see Equation (5.16)). We will not consider this further.

We contend that the correct definition of asymptotically rejoining the Hubble flow is that all the features of the test particle trajectory approach the corresponding features of the Hubble flow trajectories. Selecting one feature of the trajectory on which to base our definition is arbitrary and leads to a multitude of conflicting claims. All seven definitions have equal claim to the title of *the* definition of joining the Hubble flow. We therefore require that all definitions hold, which is equivalent to just requiring Definition 5 to hold, as it is the strongest definition. It follows that it is not a general feature of expanding universes that test particles asymptotically rejoin the Hubble flow.

Bibliography

Barnes, L., Francis, M. J., Lewis, G. F., Linder, E. V. 2005, Publications of the Astronomical Society of Australia, 22, 315

Beckwith, K. Done, C. 2004, MNRAS, 352, 353

Beckwith, K. Done, C. 2005, MNRAS, 359, 1217

Bennett, C. L., et al. 2003, ApJS, 148, 1

Book, L. 2004, http://physics.uiuc.edu/education/undergraduate/reu/2004s/Book.pdf

Bromley, B. C., Chen, K., Miller, W. A. 1997, ApJ, 475, 57

Caldwell, R. R., Kamionkowski, M., Weinberg, N. N. 2003, Physical Review Letters, 91, 071301

Carrera, M. Giulini, D. 2006, ArXiv: gr-qc/0602098

Carroll, S. M. 2004, Spacetime and geometry. An introduction to general relativity (Spacetime and geometry / Sean Carroll. San Francisco, CA, USA: Addison Wesley, ISBN 0-8053-8732-3, 2004, XIV + 513 pp.)

Carter, B. 1968, Phys. Rev., 174, 1559

Chandrasekhar, S. 1983, The mathematical theory of black holes (Research supported by NSF. Oxford/New York, Clarendon Press/Oxford University Press (International Series of Monographs on Physics. Volume 69), 1983, 663 p.)

Chodorowski, M. 2006, ArXiv: astro-ph/0601171

Cooperstock, F. I., Faraoni, V., Vollick, D. N. 1998, ApJ, 503, 61

Davis, T. M. Lineweaver, C. H. 2001, in AIP Conf. Proc. 555: Cosmology and Particle Physics, ed. R. Durrer, J. Garcia-Bellido, M. Shaposhnikov, 348–+

Davis, T. M., Lineweaver, C. H., Webb, J. K. 2003, American Journal of Physics, 71, 358

Dicke, R. H. Peebles, P. J. 1964, Physical Review Letters, 12, 435

D'Inverno, R. A. 1992, Internationale Elektronische Rundschau

Dove, J. B., Wilms, J., Begelman, M. C. 1997, ApJ, 487, 747

Fanton, C., Calvani, M., de Felice, F., Cadez, A. 1997, PASJ, 49, 159

Friedmann, A. 1922, Z. Physik, 10, 377

Gron, O. Elgaroy, O. 2006, ArXiv: astro-ph/0603162

Haardt, F. Maraschi, L. 1993, ApJ, 413, 507

Harrison, E. 2000, Cosmology : the science of the universe (Cosmology : the science of the universe, 2nd ed. by Edward Harrison. Cambridge, U.K. : Cambridge University Press, 2000.)

Harrison, E. R. 1995, ApJ, 446, 63

Hartle, J. B. 2003, Gravity : an introduction to Einstein's general relativity (Gravity / James B. Hartle. San Francisco, CA, USA: Addison Wesley, ISBN 0-8053-8662-9, 2003, XXII + 582 pp.)

Hobson, M. P., Efstathiou, G. P., Lasenby, A. N. 2005, General Relativity (General Relativity, by M. P. Hobson and G. P. Efstathiou and A. N. Lasenby, pp. . ISBN 0521829518. Cambridge, UK: Cambridge University Press, 2005.)

Hogg, D. W. 1999, ArXiv: astro-ph/9905116

Lemaître, G. 1931, MNRAS, 91, 483

Linder, E. V. 1997, First Principles of Cosmology (First Principles of Cosmology, by E.V. Linder. Prentice Hall, 1997. ISBN 0-20-140395-1.)

Melchiorri, B., Melchiorri, F., Signore, M. 2002, New Astronomy Review, 46, 693

O'Neill, B. 1995, The geometry of Kerr black holes (Wellesley, Mass. : A.K. Peters, c1995.), 54–+

Peacock, J. A. 1999, Cosmological Physics (Cosmological Physics, by John A. Peacock, pp. 704. ISBN 052141072X. Cambridge, UK: Cambridge University Press, January 1999.)

Peacock, J. A. 2006, www.roe.ac.uk/ jap/book/additions.html

Peebles, P. J. Wilkinson, D. T. 1968, Physical Review, 174, 2168

Press, W. H., Teukolsky, S. A., Vetterling, W. T., Flannery, B. P. 1992, Numerical recipes in FORTRAN. The art of scientific computing (Cambridge: University Press, —c1992, 2nd ed.)

Robertson, H. P. 1935, ApJ, 82, 284

Samuel, S. 2005, ArXiv: astro-ph/0512282

Sitnikov, L. S. 2006, ArXiv: astro-ph/0602102

Tipler, F. J. 1996, MNRAS, 282, 206

Walker, A. G. 1936, Proc. London Math. Soc., 42, 90

Weisstein, E. W. 2006, mathworld.wolfram.com/BinomialSeries.html; From MathWorld — A Wolfram Web Resource.

Whiting, A. B. 2004, The Observatory, 124, 174